AE-420
UDC 539.166
539.122.16:
539.173.4.162.2

AE-420

Energies and Yields of Prompt Gamma Rays from Fragments in Slow-Neutron Induced Fission of ^{235}U

H. Albinsson

AKTIEBOLAGET ATOMENERGI

STUDSVIK, NYKÖPING, SWEDEN 1971

ENERGIES AND YIELDS OF PROMPT GAMMA RAYS FROM FRAGMENTS IN SLOW-NEUTRON INDUCED FISSION OF ^{235}U

H. Albinsson*

ABSTRACT

Measurements were made on the gamma radiation emitted from fission fragments in slow-neutron induced fission of ^{235}U. The fragments were detected with solid state detectors of the surface barrier type and the gamma radiation with a NaI(Tl) scintillator. Mass selection was used so that the gamma radiation could be measured as a function of fragment mass. Time discrimination between the fission gammas and the prompt neutrons released in the fission process was employed to reduce the background. The gamma radiation emitted during different time intervals after the fission event was studied with the help of a collimator, the position of which was changed along the path of the fission fragments. In this way it was possible to select various collimator settings and let gamma radiation of different half-lives be enhanced. Gamma-ray energy spectra from these time components were then recorded as function of mass. The spectrum shape differed greatly depending on the half-life of the radiation and the fragment from which it was emitted.

The results of the present measurements were discussed in the light of existing fission models, and comparisons were made with prompt gamma-ray and neutron data from other fission experiments.

* Chalmers University of Technology, Gothenburg

Printed and distributed in April 1971.

LIST OF CONTENTS

1. INTRODUCTION

Prompt gamma radiation from fission fragments is of interest to study for two reasons. First, a knowledge of this radiation should be of value for any detailed theory of the fission process, and second, it can provide information for designing shielding around a reactor.

The gamma-ray energy spectra are very complicated owing to the many nuclei (fragments) which emit this radiation. Furthermore these nuclei can start emitting their radiation from states in a rather wide energy range, depending on the way in which the fragments were formed. Studies of gamma rays from fragments formed in a fission process induced by neutrons from a reactor often involve experimental difficulties, because the background at a reactor is mostly very heavy. All these problems have probably hindered a faster progress of the knowledge of prompt fission gamma radiation from the thermal-neutron induced fission of ^{235}U, and so far most studies have concerned gamma rays from fragments formed in the spontaneous fission of ^{252}Cf.

Measurements of the prompt gamma radiation have been made recently with Ge(Li) detectors on ^{252}Cf fission [1, 2], and also on ^{235}U fission [3]. The experimental technique has been improved considerably during the last five to seven years, for instance by the introduction of Si(Li) detectors, with which K X-ray energy spectra from the fragments can be recorded in a simple way [1, 2, 4-9]. These X-rays are formed through conversion of the prompt gamma rays, and studies of them can therefore yield complementary data to the knowledge of the prompt gamma radiation. Recently experiments have also been performed with X-rays and gamma rays in coincidence [1, 2, 7], and so it is now possible to determine a few of the lower gamma-ray cascades in some mass regions.

The main difference between the present experiment and most others reported so far is the use of a collimator to select different time intervals after the fission event. This technique has been used in few experiments up till now [10-13]. The present study follows in basic principle the ideas outlined by Johansson [10]. With the collimator it is possible to study the time distribution of the gamma radiation, such as decay curves of the integral radiation from all fragments or from certain fragments, and also to record gamma-ray energy spectra from certain fragments during different time intervals after the fission event. This means that gamma radiation of different half-lives as a function of fragment mass can be studied.

Another interesting parameter in these investigations is the total fragment kinetic energy. This will be reported separately [14]. The data acquisition system was a two-parameter analyzer, so that there is simply no possibility to add more parameters to the two whose inter-relations were studied: gamma-ray energy and fragment mass.

It is sometimes possible to use more than one existing model in nuclear physics for the interpretation of fission data. One often used model is the collective model, the reason being of course that the fission process is really a collective, many-particle process. Some extra problems arise, however, as the fragments, just after their formation, are very neutron-rich, and it may be difficult to compare results of fission gamma-ray studies with those of other nuclear reactions. Of great interest for purposes of comparison are the data from prompt neutron emission studies, and quite a lot of the discussion from these studies can be adopted for the interpretation of prompt fission gamma radiation. Unfortunately the situation surrounding prompt neutron emission is far from clear, and it seems as if more effort will have to be

put into the studies of the prompt decays of the fragments.

The gamma radiation studied in the present work is the part which is characterized as prompt. Somewhat arbitrarily the radiation is usually divided into two parts, namely a prompt part whose components have half-lives shorter than 1 ns, and a delayed part with longer half-lives. This division is further justified by the fact that the experimental techniques for study of the two parts differ and that the properties of the radiation in the two cases show a distinct difference [10].

In the present experiment a special technique was adopted, namely that of using time-of-flight discrimination between the prompt neutrons and the fission gamma radiation. This was done by placing the gamma detector about 70 cm from the fission foil. This technique has not been used extensively so far, probably because of the small solid angles involved and, as a consequence, the low counting rates in the gamma detector [12, 13, 15-17].

2. EXPERIMENTAL PROCEDURE

2.1. Apparatus

Fig. 1 shows a block diagram of the electronics used in this experiment. The details of the design and the system performance have been discussed recently [18], and it will suffice to describe briefly some of the specific features of this set-up.

The fissile deposit was 1 cm^2 in area and prepared by electrodeposition on 100 $\mu g/cm^2$ nickel foils. The thickness of the uranium layer was about 100 $\mu g/cm^2$ in order to allow measurements of mass spectra with acceptable resolution. Two solid state detectors of the surface barrier type were placed in parallel and symmetrically around the foil

to measure the energies of the fission fragments. The detectors* were about 4 cm^2 in area, fabricated from 400 ohmcm n-type silicon and operated at about 70 V bias. The distance between each detector and the fissile foil was 2 cm. The gamma detector was a NaI(Tl) scintillator, 10.4 cm long and 13.0 cm in diameter, viewed by a Philips XP 1040 photomultiplier tube. The associated electronics**, consisting of a pulse-shaping unit and a discriminator, was coupled directly to the photomultiplier tube socket and gave a fast leading-edge time pulse and a linear pulse.

Pulses from the solid state detectors were amplified in charge-sensitive preamplifiers followed by linear amplifiers.

The amplified pulses were then fed into a linear divider circuit which performed the operation of dividing one pulse by the sum of both. By disregarding prompt neutron evaporation and energy losses in the target material, it can easily be shown that the ratio of the energies of the two fragments is inversely proportional to the mass ratio. Consequently, if E_1 and E_2 are the kinetic energies of the respective fragments and M_1 and M_2 are the associated mass numbers, one readily gets

$$\frac{E_1}{E_1 + E_2} = \frac{M_2}{M_1 + M_2} \propto M_2$$

i.e. the spectrum from the output of the divider circuit is simply the mass spectrum. As distinguished from an earlier divider circuit [18], which was mainly a logarithmic amplifier, the present divider circuit was linear***.

---

* Type C7904 Heavy Ion Detectors supplied by ORTEC, Oak Ridge, Tenn., USA.

** Designed and built at the Research Institute of National Defence, Stockholm [19].

*** Designed and built at the Physics Department, University of Lund, Lund, after an idea presented by Gere and Miller [20].

In all these measurements a NaI scintillator was used for gamma radiation detection due to its high efficiency. As the counting rates are very low, it was found to be more important to detect as many events as possible than to get high resolution but low efficiency, as with a Ge(Li) detector.

A lead collimator, movable in parallel with the direction of the detected fragments and also with a variable slit, was used to select gamma radiation in different time intervals after the fission event.

The data recording system was the same as in ref. [18], namely a two-parameter analyzer, the memory of which was that of a small computer, PDP-8/S.

2.2. Performance

As will be demonstrated in some figures in the following section, the resolution of the gamma peaks is in general very poor. The reason for this is that a NaI scintillator has been used for gamma detection instead of a Ge(Li) detector, and furthermore that the gamma radiation has been accumulated as function of mass groups rather than single masses. The reason for measuring in this way was discussed briefly in an earlier paper [18], and some additional arguments will now be presented which are pertinent mainly to the gamma-ray energy spectra which are the subject of the present study.

That the resolution of the gamma-ray spectra is poor need not necessarily be a serious drawback in the present studies, as one can obtain a lot of information about the excitation of the fragments without doing any "normal" nuclear spectroscopy. As has been discussed by Johansson [10], the fragments de-excite mainly through vibrational cascades just after the prompt neutron emission, and these transitions

seem to be similar for all fragments. Instead of presenting level schemes for individual fragments, one can calculate and show yields of photons in specific energy regions as function of fragment mass and thus study gamma-energy variations over the mass spectrum. These yield functions have been calculated by summing up the number of recorded photons in specific gamma-ray energy portions and then dividing these functions by the yield of the mass spectrum.

There are many ways of making the summation, depending on the gamma-ray energy regions of interest, and the interest usually arises gradually when studying the behaviour of the gamma-ray energy spectra. Several of these yield functions will appear in the following section.

3. RESULTS

3.1. General

The gamma-ray energy spectra of all prompt fission gammas is presented in fig. 2. It was recorded in coincidence with the gammas of the time-of-flight spectrum and no lead collimator was used. The over-all background is less than 1 %. No corrections have been made for the response function of the detector, because the only intention in presenting it here is to demonstrate its general appearance and the similarity to the same spectrum recorded earlier, for instance by Mainschein [21]. The latter reference contains a review of these types of spectra together with theoretical comparisons. The shape of the spectra has often been fitted to analytical expressions, and the spectrum in fig. 2 fits well into those expressions. But the analytical equations have no significance from the fission physics aspect other than that they might be used in reactor shielding calculations [21].

As mentioned above, the gamma-ray energy spectrum in fig. 2 is

very complex, but some details can be obtained through certain procedures. One procedure is to record the gamma spectra in coincidence with the mass spectrum in a two-parameter analyzer, and another, which can also be used together with the first one, is to select certain time regions after the fission event by use of a lead collimator. The collimator will then enhance gamma radiation with a certain half-life, and figs. 3 and 4 show examples of such gamma-ray energy spectra. The enhanced radiation has a half-life of about 50 ps and the spectra are integrated over the whole mass spectrum. The only difference between figs. 3 and 4, as seen, is the gamma-ray energy range. Comparison of the figures of these two spectra with the spectrum in fig. 2 shows very clearly that the structure of the "whole" spectrum in fig. 2 can be revealed by proper use of a collimator. For the respective half-lives the different fragments, in turn, can give very different spectra. It might be mentioned at this point that mass separation is not fully effective without the collimator, because the mass spectrum is obtained by dividing the fragment energy pulse heights electronically. In a certain fission event, however, the gamma detector can never tell which of the two fragments emitted a recorded photon, unless one of the fragments has been shadowed by a collimator.

3.2. Gamma rays associated with half-lives of about 50 ps

One series of measurements, consisting of the accumulation of gamma-ray energy spectra as function of mass, were recorded for a time interval after fission corresponding to a fragment flight path of 2 to 15 mm. The half-life of the radiation enhanced with this collimator setting was 50 ps and more. The average velocity of the fragments is about 1 cm/ns, and this collimator setting means that the time interval

covered after fission is 0.2 - 1.5 ns on the average. The length of the collimator is about 13 cm and therefore there is about 1 mm more on both sides of the studied flight path which is seen by the gamma detector. Anyway, with this collimator setting the prompter half-lives of the gamma radiation have very low intensities, even if it may be said that the experiment might not have been optimized as far as the intensity is concerned. This collimator setting was chosen so as to reduce the background in the recorded gamma-ray spectra, due to faster radiations, to a very low level, namely less than 5 %. The main contribution to the background was the general reactor background and amounted to less than 20 %.

The measurement was performed in two steps covering the gamma-ray energy ranges of 0 - 4.2 MeV and 0 - 0.8 MeV respectively. The integrated gamma spectra with no mass selection are those shown in figs. 3 and 4, and examples of mass-sorted spectra are presented in fig. 5. The division of the gamma-ray energy portions was performed somewhat arbitrarily, but with the aim, if possible, of resolving gamma lines in the two regions in the most effective way with regard to the resolution of the detector and the number of channels available in the data recording system. In the spectrum covering energies up to 4.2 MeV it is impossible, even theoretically, to resolve lines of gamma rays of energies less than about 0.5 MeV. On the other hand it should be possible to resolve peaks in the energy region 0.5 to 2 MeV, while peaks in regions of higher energies should appear as broad bumps, unless they are very intense.

The spectra in fig. 5 are from the raw data, and the absolute intensities of each curve have not been corrected for the mass distribution.

The 1.2 MeV bump is present in several gamma-ray spectra and

will therefore be presented under a separate heading in this chapter.

Gamma rays of energies around 200 keV have been found in a considerable proportion in some mass regions. The relative yield of such photons as a function of fragment mass is shown in fig. 6. This function is seen to be strongly mass-dependent and has a sawtooth type appearance.

The relative number of gamma rays of energies in the region of about 400 to 800 keV is also mass-dependent, as can be seen from fig. 7. The shape of this curve will be considered in detail in the discussion, but it is noticeable that it looks similar to the corresponding yield of photons of energies around 1200 keV (fig. 8).

The selection of energy region is a very important task, and one must be very careful in drawing conclusions from the above-mentioned results. To illustrate the problem a little, fig. 9 has been included. To obtain the yield presented there, namely the relative yield of photons with energies less than about 400 keV, a summation of the number of counts was made for the first ten gamma-ray energy channels in the spectra of gamma-ray energies between 0 and 4.2 MeV as function of fragment mass. The relative yield covered goes from about 1 to 4 in this figure, while in fig. 6 it goes from about 1 to about 2.5. It might seem self-explanatory that the yield ranges should be different, because the energy regions covered are not the same; but when starting the analysis one may be tempted to overlook this significance, as the recorded spectra do not differ too much except as regards the yield of the 200 keV photons. These yield curves, however, clearly show that there is more difference in the spectra than just the photons of lowest energy.

One reason for choosing such a wide gamma-ray energy range as

up to 4.2 MeV was to look for possible octupole transitions. With this collimator setting, which enhances radiation with a half-life of about 50 ps and more, one can estimate that the corresponding collective octupole radiation has an energy of about 2 - 3 MeV. There are reasons to believe that these radiations should exist as a result of the breakup of the fissioning nucleus. Besides quadrupole-shaped, pear-shaped fragments might be formed and the asymmetric part of the latter nuclei would be sloshing back and forth. Unfortunately no clear evidence of such radiations was found, for the main part probably because of intensity reasons. The recorded number of counts per channel was low in these gamma-ray energy portions.

3.3. Gamma rays associated with half-lives of about 20 ps

One series of measurements was performed with a 1 mm wide collimator slit placed so close to the fission foil that radiation with half-lives around 20 ps was enhanced. The gamma-ray energy spectra do not differ very much as a function of the fragment mass investigated, even though a small difference does in fact exist, as can be found from a closer analysis (fig. 10). Differences can be observed, however, by studying the yields of photons of certain energies as function of fragment mass. One study covered the energy region from about 0.2 to 2.0 MeV. The yield curve of all those photons is shown in fig. 11 together with yield curves for specific gamma-ray energy portions.

In all gamma-ray energy spectra a broad distribution of photons has been found, with energies from about 200 to 1800 keV and, especially in mass regions around 105 and 145, an abundance of 400 keV photons superposed over the broad distribution.

Two measurements were performed with this collimator position,

but with different gamma-ray energy ranges. One was the above-mentioned study covering 0.2 to 2.0 MeV and the other covered 70 to 700 keV. Where the two measurements overlap in gamma-ray energy, the relative yield curves of the number of photons are identical within the error limits.

The general background in the time-of-flight spectra was about 15 %. The signal-to-background ratio was normally an increasing function with gamma-ray energy in the present set-up [22] and for energies above about 400 keV the background was about 10 % or less.

One may argue that the collimator slit width in this measurement was too wide; and even if gamma radiation with a half-life of 20 ps was mainly enhanced, there could be a considerable contribution of slower radiation as well. However, by studying the shapes of the gamma-ray spectra and also the yield curves of the number of photons as function of fragment mass, one is readily convinced that the contribution of slower radiation, i.e. mainly with $T_{1/2}$ = 50 ps, must be quite small. The adjustment of the collimator for the enhancement of the $T_{1/2}$ = 50 ps radiation is very easily done, and consequently the shapes of those gamma-ray energy spectra are well known.

The distribution around 200 keV from the heaviest fragments in each mass group are probably coming from the above-mentioned 50 ps component. The intensity of those bumps in fig. 5 are roughly equal to what can be estimated from the intensity distribution of each of these two components [22].

3.4. Gamma rays associated with half-lives of about 7 ps

Measurements of gamma radiation with a half-life of about 7 ps are very difficult to perform mechanically. Some of the difficulties

have been described briefly in ref. [22]. One measurement was done with a gamma-ray energy window covering about 0.2 to 2.0 MeV. The integrated gamma-ray energy spectrum is shown in fig. 12. There it can be seen that the recorded spectrum is a broad distribution centered around 1 MeV. Examples of mass-sorted spectra are shown in fig. 13. There is not much difference between them; there is a slight shift in medium energy, so that the average gamma-ray energy is slightly larger over the heavy mass peak than over the light one.

The relative yield of photons within the whole gamma-ray energy range is typically of the sawtooth type as demonstrated in fig. 14. More limited gamma-ray energy portions show in general the same behaviour, even though the yield curves differ in details.

3.5. The uncollimated gamma radiation

One short measurement has been devoted to the study of gamma-ray energy spectra as function of the fragment mass ratio. The gamma-ray spectra appear in two groups, but one spectrum in one group should have a correspondence in the other group. The two groups, of course, resemble the mass spectrum. It should therefore be possible to add the two corresponding spectra to one spectrum in order to improve the statistics. This has been done in a few cases. Of particular interest has been that the 1200 keV photons are enhanced for the mass combinations around 104 + 132, and this bump stands out very clearly for mass combinations around these mass numbers (fig. 15). The 1200 keV photons will be treated under a separate heading.

3.6. The 1200 keV distribution

In the integrated gamma-ray spectrum (fig. 2) one notices the

presence of a small bump around 1200 keV. This bump has not received any particular attention earlier, even though it can be seen in the first fission gamma-ray spectra presented, for instance, by Maienschein. The reason for the lack of its discussion is probably that it is not very pronounced and that spectra covering energy ranges of more than 1 MeV have seldom been recorded earlier as function of mass. As the 1200 keV gamma rays show up both in spectra in which the 7 ps and in which the 50 ps half-life is enhanced, the bump deserves some special attention.

First one must be convinced that these gamma rays come from fission fragments and not from background. This is, of course, not at all clear from the integrated gamma-ray spectrum (fig. 2). The relative yield of 1200 keV photons, however, has been found to be a function of fragment mass (fig. 8), and so one has a firm ground on which to base the assumption that the 1200 keV gamma rays come from the energy release of particular fragments. The largest yield was found for the lightest mass in the heavy and light mass groups, respectively, but a broad bump also appears around mass number 95. There is a tendency to an increase in yield for mass numbers above 145, but the number of recorded photons was very low and therefore the yield value contains a large error in that mass region. The structure between mass numbers 80 and 95 is noteworthy and will be dealt with in the discussion. The yield, especially from the radiation with the 50 ps half-life, and its mass dependence, will be discussed in greater detail later on.

As has been discussed earlier [18], with the present technique there is no possibility of resolving individual lines in the gamma-ray spectra, as the mass dispersion is too poor. On the other hand this limitation need not be too much of a drawback. Instead one can take

advantage of the high efficiency of this type of gamma detector as compared to the low efficiency but high resolution of, for example, a Ge(Li) detector.

4. ANALYSIS OF THE DATA

4.1. Comparisons with prompt neutron data

It has been pointed out earlier that the prompt fission gamma radiation exhibits features which in many respects are unusual compared to those of the radiation in other reactions. On the assumption that the gamma emission can occur only after the prompt neutron emission is energetically impossible, a total energy release in the form of gamma emission may be calculated at about 5 MeV [23]. The total energy is, in fact, about double this figure and the discrepancy is nowadays explained as being due to decays from high-spin states [10, 24].

In the interpretation of the results of the present measurements it is plausible to introduce arguments given when discussing the yield of prompt neutrons from fission fragments, as the gamma radiation follows the neutrons. There are several reasons, however, to be very careful in making such comparisons. Studies of prompt neutrons are beset with considerable experimental difficulties, as the neutrons can only be assumed to be emitted from moving fragments with a certain amount of probability. Several experiments have shown that, depending on the fissioning nucleus, a considerable fraction of the prompt neutrons is also emitted at the instant of scission. Nowadays one makes a clear distinction between the two types of neutrons. The term fragment neutrons is used to describe the neutrons emitted from the fragments, whereas scission neutrons or central neutrons describe the neutrons appearing at scission. It has been concluded that, on average, 85 - 90 %

of the neutrons in uranium fission are emitted from moving fragments [25, 26]. In a detailed description of the de-excitation of the fragments this fact must be taken into account. It has recently been estimated that in an event in the thermal fission of ^{235}U, resulting in a total kinetic energy of about 190 MeV, about one half of the total number of the emitted neutrons are scission neutrons [27]. This has given rise to some interesting discussions about the excitation energies of the fragments.

As is well known, the yield of prompt neutrons decreases as the fragment total kinetic energies increase. When the total kinetic energy has its maximum, it is also known that it is associated with a nearly asymmetric fission event. According to Maslin et al. [28] the average number of prompt neutrons emitted is then about 1.2 and so, according to Blinov et al. [27], there would be no more than about 0.6 fragment neutrons emitted per fission event. The average number of prompt neutrons in all uranium fission events is about 2.4. As mentioned above, several experimentalists have reported that about 85 - 90 % of these are fragment neutrons, which means that about 0.3 neutrons per fission event are scission neutrons. It cannot be stated that the number of scission neutrons should increase, as it seems here, from 0.3 to 0.6 when the total kinetic energy increases. One can only assume that a fission event resulting in the highest kinetic energies may arise from a more than "normally" violent process. In general it is believed that the scission neutrons are emitted at the time of scission because of disturbance associated with the breaking of the neck and the consecutive retraction of the stumps into the fragments [29, 30]. The high total kinetic energy may result in a lower than expected average number of fragment neutrons. Another possibility, however, is that the high total kinetic energy is associated with a higher than average initial

spin value of the fragments, which may constitute a hindrance factor, and instead the gamma decay will be enhanced. Problems associated with the total kinetic energy have been discussed in detail elsewhere [14].

A complete discussion of the fission gamma decay can therefore hardly be based on the fragments emitting all the prompt neutrons and the consecutive decay coming in the form of gamma emission. These two decays are, of course, linked together, neutron decay being the faster, followed by the gamma decay. As mentioned earlier, the initial spin distribution of the fragments will then be one of the "means" through which the fragments select their decay modes.

Some of the features of the yield curves in figs. 6 - 9, 11, 14 showing the relative number of photons as a function of fragment mass for the different half-lives can be interpreted on the same basis as discussed in an earlier work [18]. The important physical idea behind this interpretation is that the fragments are more or less susceptible to deformation, depending on whether they consist of closed nucleon shells or not. This idea was put forward by Vandenbosch and Terrell [31, 32] and has been very successful in interpreting data on de-excitation of fission fragments. Most of the excitation energy of the fragments is, according to this idea, taken up by deformation directly after the scission act. A spherical nucleus, with one or both nucleon shells closed or almost closed, is resistant to deformation and its initial excitation energy should not be so high as in a nucleus which can easily be deformed, i.e. with one or both of its nucleon numbers far from being magic. The sawtooth curve reflecting the yield of prompt neutrons and also the yield of prompt photons as a function of fragment mass is well described by this model.

As far as the prompt gamma radiation is concerned, it is well interpreted according to this model. It has often been assumed that the prompt neutron is the result of an evaporation, and in a first simple approximation one often describes the prompt neutron emission in terms of a Maxwellian spectrum. It is known, however, that the prompt gamma emission can compete with the prompt neutron emission at excitation energies well above the binding energy of the neutron in the fragments, and this effect seems to be the result of the spin distribution.

4.2. Fragment spin and gamma-ray energy yield

The spin distribution of the fragments has not been measured in this work. As the spin plays an important role in the de-excitation of the nuclei, some of the spectra will be discussed on the basis of what is known today about it.

One of the latest papers on the initial spin distribution of the fission fragments is that by Armbruster et al. [33]. An average value of seven units of angular momentum was obtained, which increased strongly within each fission mass group from values of about 5 - 10 units of angular momentum. Another interesting conclusion drawn by Armbruster et al. was that the de-excitation mechanism of the fission fragments is not governed by the level density following from a statistical model, but that the fragments mainly de-excite by emission of quadrupole radiation from stretched collective cascades. This idea has also been put forward earlier [10, 24].

It is interesting to study the relationship between the average energies of the main groups of the gamma rays in the three spectra and their associated half-lives. Such a study may yield information which can form a basis for interpretation of the type of gamma radiation in-

volved. It was found that the time component with a half-life of about 7 ps was associated with a broad bump in the gamma-ray energy spectrum around 1100 keV, whereas for the 20 ps component there was an abundance of photons around 800 keV, and for the 50 ps component the photon yield was very large around 200 keV. In a plot of the logarithm of the half-life as a function of the gamma-ray energy in the three cases mentioned above, namely (200 keV, 50 ps), (800 keV, 20 ps) and (1200 keV, 7 ps), these three points will fall in a region having values taken from data sheets for the energy of the lowest excited 2^+ levels and their corresponding half-lives for gamma decay in even-even nuclei. This could be a strong indication that collective quadrupole radiation constitutes a very great part of the prompt fission gamma radiation, i.e. the same conclusion as arrived at by, for instance, Armbruster et al. [33] in their measurements, and also suggested by Johansson [10].

As mentioned in the previous section and also discussed above, a considerable difference seems to exist in the shapes of the gamma-ray energy spectra, depending on whether the 7, 20 or 50 ps half-lives were enhanced. The paper by Armbruster et al. [33] presents a figure showing that the gamma-ray energy spectrum for the uncollimated beam is practically the same, as far as the shape is concerned, as the one with the collimator selecting photons in the time region 10 - 100 ps after scission. This collimator setting means that the 20 ps half-life component is enhanced, which can be easily checked by studying fig. 6 in Johansson's work [10], which concerns ^{252}Cf fission. The present work on ^{235}U fission gives a similar intensity distribution leading to a half-life of about 20 ps. Johansson presented gamma-ray energy spectra with the collimator set to enhance radiation in practically the same time interval, 10 - 70 ps. In Armbruster's work the corresponding

time interval was 10 - 100 ps, which should not give any significant difference in the energy spectra because the intensity distribution is a strongly decreasing function with time after scission, and so the extra 30 ps from 70 to 100 ps should not make much difference. The energy spectra in the present work resemble those presented by Johansson [10] when this time component was enhanced, but the broad distribution of photons with energies around 800 keV seems to have no similarity to the spectra presented by Armbruster et al. [33]. The collimator setting used in the present work was practically the same as the one used by Armbruster et al. [33]. Moreover, the energy spectrum recorded without the collimator by Armbruster et al. does not look the same as the one presented in ref. [18], whereas the uncollimated spectrum from the present work does. Unfortunately Armbruster et al. did not comment on this matter in their paper, as the main object of their work was to study the primary spins of the ^{235}U fission fragments.

4.3. Comparisons with gamma-ray data from ^{252}Cf fission

A few recently published papers have given the half-lives of some gamma transitions in ^{252}Cf fission [1, 2, 6]. Several of these half-lives are of the order of nanoseconds and the associated energies are around 100 keV. Some of the measurements were performed in such a way that the energies of coincident internal conversion electrons and K X-rays were recorded. In one of the most recent reports giving data on the ground-state bands of nuclei in the mass region around 100, information is given which at first glance should be of great value for the interpretation of the present results. Differences exist, however, in the ways in which the present and the californium measurements have been performed. The californium work included studies of K X-rays, and therefore a

certain selection of the transition type has been made. X-rays formed as a result of conversion are favoured for the lower gamma-ray energies. The californium work has resulted in a set of gamma-ray energy values and associated half-lives, especially in the mass region around 100, where predictions for ground-state rotational bands have been given with great confidence. Gamma-ray energies and half-lives were also given, however, for many other low-energy photons from fragments elsewhere along the mass distribution of the spontaneous fission of ^{252}Cf. A direct comparison cannot be made in all respects between the present data and those of the ^{252}Cf work. As far as the radiation of $T_{1/2}$ = 50 ps and more is concerned, several of the gammas found around 200 keV in the present work are probably the same as those found in the californium experiments.

The Karlsruhe measurements [3] concern thermal-neutron induced fission of ^{235}U, and the results in the form of gamma lines show that there are several similarities between californium and uranium fission. The Karlsruhe as well as the Berkeley group used a Ge(Li) detector and therefore obtained a set of gamma lines of well defined energies, especially in the low energy portion. The energies found in the uranium work very often coincide with those of the californium studies, and therefore one may assume that several of those lines are the same as those of the present measurement. Most of these lines have been found in mass regions around the heaviest masses in each mass group, where fragments easily susceptible to deformation are expected to occur. They may then originate from the slowest time component.

4.4. Gamma rays of energies around 1200 keV

The 1200 keV photons deserve special attention in this analysis.

From the results of the present measurements it is clear that these gammas play a very important role in the de-excitation of the fragments, and in fig. 3 the broad distribution stands out very clearly. In the mass-sorted spectra the 1200 keV photons show up mostly in mass regions around 82, 94 and 130. Of particular interest is that the relative yield of gamma rays of energies in the region 400 - 800 keV is a similar function, except that the yield is low from the very lightest fragments. This yield curve was obtained with the same collimator setting as that for the 1200 keV photons. No specific conclusion should be drawn from this fact, even though it is tempting to venture the guess that these gamma rays form part of a cascade. With a slightly different collimator setting one would have seen a difference in the respective relative intensities of these gamma rays, and from this difference it would be possible to calculate whether and how these gamma rays are associated in a cascade. The difference in gamma-ray energy would be associated with a consecutive difference in half-life, the 1200 keV being the faster decay.

The gamma-ray energy spectra in the mass regions showing an abundance of the 1200 keV also show a slight shift towards higher energies in the average gamma-ray energy for the photon distribution in the energy portion of less than 400 keV (fig. 16). The 1200 keV gamma rays may therefore be associated with gamma rays of energies of around 300 keV. That the 1200 keV gamma rays are present in the spectra where the 50 ps half-life gamma component is enhanced is an extraordinary feature. On the assumption that the 1200 keV gamma rays are of the collective quadrupole type, one would assume a half-life of no more than 10 ps, and the 1200 keV photons would never be recorded with any measurable intensity with this collimator setting. There are therefore

reasons to believe that the 300 keV photons precede the 1200 keV photons in a cascade, and that the collimator setting is suitable for detecting the low-energy photons, whereas the 1200 keV photons are delayed. A slightly different collimator setting would be of great help in indentifying this proposed cascade. As was suggested by Johansson [10], one may assume the possibility of a vibration of the beta type among the stiff fragments with mass numbers around 82 and 132, from which fragments the 300 and 1200 keV photons appear in greater abundance than elsewhere.

The 1100 keV gamma rays appearing in the spectra for which the 7 ps half-life is enhanced are probably of more normal vibrational type. The relative yield of these gamma rays is a typical sawtooth function and reflects directly the excitation energies of the fragments soon after the prompt neutrons have been emitted. They must be among the first members of the gamma cascades, and their relative yields from mass to mass depend on the relative excitation energies of the fragments. When the collimator is set to enhance gamma radiation with a half-life of about 20 ps, the 1200 keV gamma rays have low yields compared to the photons of energies of 800 keV and below. When the 50 ps half-life is enhanced, most of the yields of photons are of energies around 200 keV from the heaviest fragments in each mass group, whereas the 1200 keV photons have low yields compared to the 200 keV photons, but still of the same order as the associated 300 keV photons.

4.5. Average gamma-ray energies

The average energies of the gamma rays were estimated in some of the gamma-ray energy spectra. In the case when radiation of half-life $T_{1/2}$ = 7 ps was enhanced, the variation of the average gamma-ray

energy with fragment mass was within about 0.1 MeV, with the highest energies for the lightest fragments in each mass group and the lowest energies for the heaviest fragments (fig. 17). A similar calculation for the radiation of half-life $T_{1/2}$ = 20 ps showed a similar curve with the average energy around 0.85 MeV (fig. 18).

Maier-Leibnitz et al. [34] arrived at the conclusion that the uncollimated radiation showed no essential dependence on mass. The average energy in the mass region around 130, however, was appreciably higher than in other mass regions, namely around 4 MeV. The present measurement and that of Maier-Leibnitz et al. have been performed in different ways, and the average photon energies estimated in this study are smaller for masses around 130 than those obtained by Maier-Leibnitz et al. The aim of the present work has been to study the gamma-ray energies as function of mass and time after fission, and therefore gamma-ray energy portions have been selected bearing in mind previous knowledge obtained from the work of, for instance, Maier-Leibnitz et al. Figs. 17 and 18 only show where the bulk of the gammas in these energy spectra are centered, i.e. they tell which average energy is associated with most of the photons emitted when the radiations of $T_{1/2}$ = = 7 and 20 ps, respectively, are enhanced.

It is reasonable to assume that, if a gamma-ray energy portion of about 10 MeV had been studied, i.e. as in fig. 2, the average gamma-ray energy for the whole spectrum would vary more in fig. 17 and 18. Such a measurement should be performed, as it would result in a total gamma-ray energy release associated with the half-lives of 7 and 20 ps. In the present work this measurement was omitted because of lack of time. In principle such a measurement differs from the one performed only in the respect that the gamma-ray energy range of the data re-

cording system should be differently chosen.

When an estimate of the average photon energy has been obtained, and also the relative yield of photons as a function of fragment mass, one can qualitatively get the variation of the energy release of the fragments in the form of gamma radiation in the respective time regions studied in the present work. As far as the 7 and 20 ps components are concerned, the respective average gamma-ray energies vary but little from one mass region to another, and the average energy release in the form of gamma radiation as a function of fragment mass will be a curve of the sawtooth type. A rough estimate of the total energy release within the first one-tenth of a nanosecond would give an average for the light and heavy mass groups of about 3 MeV, with a sawtooth variation in each mass group going from about 1 to 5 MeV. By studying the decay curve of the prompt fission gamma radiation one finds that at least 75% of the total energy has been released within this time region, and this value agrees rather well with the accumulated yields mentioned by earlier authors [10, 35].

4.6. Possible octupole vibrations

During recent years more and more attention has been paid to octupole vibrational states in deformed nuclei [36 - 39]. It is reasonable to expect these states to be formed also in fission fragments as, just after scission, there is a large probability that easily deformable fragments may assume shapes resembling pears. Recent calculations, which agree well with experimental results, give energies for the first 3^- states in the rare-earth region of about 1.5 MeV [39]. As far as the energies are concerned, the 1^- states could coincide with the 1.2 MeV photons, but the yield curve of those photons is in disagreement with this picture,

as the 1.2 MeV photons are mainly released from nuclei containing closed or almost closed nucleon shells. On the other hand it is reasonable to expect the E3 transitions from the 3^- states to be of the order of 2 MeV. A calculated yield curve, however, covering the gamma-ray energy region of about 1.6 to 2.4 MeV, as a function of fragment mass showed practically no variation over the whole fragment mass distribution. Studies of other energy portions up to about 4 MeV showed very little variation with mass.

As far as the heaviest fragments are concerned, one may expect their lowest octupole states to have excitation energies of about 1.2 to 1.5 MeV, and the yield curve of the 1200 keV photons as a function of fragment mass (fig. 8) there is indeed the beginning of an increase in yield when the mass number goes from 145 and upwards. Unfortunately the number of counts is not very large and it is not possible to state, or even assume, anything indicative of the presence of this kind of radiation in that region.

The half-life of this radiation is expected to be larger than that of the quadrupole radiation, and in a future experiment, one should be able to select this radiation by using a narrower collimator slit. The collimator could first be positioned at the "beginning" of the time interval chosen in the experiment presented here. With the same narrower collimator, but placed further away from the foil, one can then get the slower radiation enhanced and very little contribution from the quadrupole radiation, and the variation in intensity between the two types of radiation would come out clearly.

5. DISCUSSION

One may remark that the yield curves presented do not show up

so much structure as the one presented in an earlier work [18]. The collimator settings were, however, slightly different from the one used in ref. [18], as in the present work the settings were chosen carefully to allow enhancement of the two time components with half-lives of 7 and 20 ps. As mentioned in ref. [18], the selected time interval was 10^{-11} - 10^{-10} s, but it was found later that the 10^{-10} s limit was slightly higher, so that the intensity of the 20 ps component was decreased relatively more than that of the 50 ps time component. In the present work the gamma-ray energy ranges were limited to the first two MeV, which should have some, though a small, effect, whereas in the earlier work there was no limit on the gamma-ray energy portion selected.

As has been mentioned earlier [18], the resolution of the gamma detector is about 10 %. Since several fragments can contribute to one gamma-ray energy spectrum, it is impossible with this system to resolve single gamma lines in a spectrum. The mass resolution is about 4 - 5 amu [18] and it is no use trying to look for single lines which might belong to specific fragments. It may be remarked, for instance, that within the mass regions where the nuclei seem to have deformed shapes, the variation in mass number of 4 - 5 amu may change the energy of the first 2^+ levels in even-even nuclei by about 10 keV. Bearing this in mind it is easy to understand that the distributions around 200 keV in the gamma-ray spectra of figs. 4 and 5 probably come from decays of several fragments.

The inherent bad resolution of this system was of course known when the present studies started, but, as mentioned earlier [18], the aim of this work has been to study gamma-ray yields as function of fragment groups and time of fission. For physical reasons this can be acceptable, as the energy of the gamma radiation from rotational and vi-

brational cascades varies slowly with mass number in regions of deformed nuclei. Even though a unique determination of the fragment mass number could be made, the charge dispersion is not known very accurately.

6. CONCLUSIONS

Studies have been performed of the gamma radiation from fission fragments in slow-neutron induced fission of ^{235}U. Gamma-ray energy spectra were recorded as function of mass and time after fission. The main conclusions from the investigation may be summarized as follows:

1. The gamma-ray energy spectra vary in shape with time after fission.

2. The gamma-ray energy spectra vary in shape with mass within each time interval, the variation being stronger the later the time interval studied.

3. When a time interval is selected in which half-lives of the radiation of 50 ps and more are enhanced, there is a strongly mass-dependent yield of 1200 keV photons, which might come late in a cascade of gammas.

4. There is a very strong dependence on mass of the yield of photons of a few hundred keV in the time interval in which half-lives of 50 ps and more are enhanced.

5. The relationship between the average gamma-ray energies and the associated half-lives gives a strong indication that the bulk of prompt photons from fission fragments are of the quadrupole type.

6. Yield curves of the photons as function of mass can be interpreted on the basis of a model including the property of the varying resistance to deformation of the nuclei, depending on whether they contain nucleons of magic numbers or not.

Investigations in this field are in progress at various laboratories, which will add to the information on excited states in nuclei far from the line of beta stability. It is hoped that, with some luck, it will also be possible to make some contributions to the understanding of the fission process.

ACKNOWLEDGEMENTS

It is a great pleasure to thank Professor S. Johansson for valuable discussions and Professor N. Ryde and Dr. T. Wiedling for their interest in this work. The assistance from Mr. L. Lindow is gratefully acknowledged. Many thanks are due to Mr. E. Karlsson for building the divider circuit.

REFERENCES

1. CHEIFETZ E. et al.,
Experimental information concerning deformation of neutron rich nuclei in the A $\sim$ 100 region.
Phys. Rev. Lett. 25 (1970) p. 38.

2. WILHELMY J.B. et al.,
Ground-state bands in neutron-rich even Te, Ba, Ce, Nd, and Sm isotopes produced in the fission of ^{252}Cf.
Phys. Rev. Lett. 25 (1970) p. 1122.

3. HORSCH F. and MICHAELIS W.,
Prompt gamma rays emitted from individual fragments in neutron-induced fission. Physics and chemistry of fission.
Proc. of a symp. Vienna, 28 July - 1 August 1969.
IAEA, Vienna, 1969, p. 527.

4. KAPOOR S.S., BOWMAN H.R., and THOMPSON S.G.,
Emission of K X-rays and division of nuclear charge in the spontaneous fission of ^{252}Cf.
Phys. Rev. 140 (1965) p. B1310.

5. WATSON R.L., BOWMAN H.R., and THOMPSON S.G.,
K X-ray yields of primary ^{252}Cf fission products.
Phys. Rev. 162 (1967) p. 1169.

6. WATSON R.L. et al.,
A study of the low-energy transitions arising from the prompt de-excitation of fission fragments.
Nucl. Phys. A141 (1970) p. 449.

7. RUEGSEGGER, Jr., D.R. and ROY R.R.,
Gamma rays in coincidence with K X-rays from the La, Ce, and Pr fission fragments of Cf^{252}.
Phys. Rev. C 1 (1970) p. 631.

8. WATSON R.L., JARED R.C., and THOMPSON S.G.,
Distribution of K X-rays as a function of mass and atomic number in the spontaneous fission of ^{252}Cf.
Phys. Rev. C 1 (1970) p. 1866.

9. KATARIA S.K. et al.,
K X-ray yields in 0 - 1 μs from ^{236}U fragments.
Nucl. Phys. A154 (1970) p. 458.

10. JOHANSSON S.A.E.,
Gamma de-excitation of fission fragments. (I). Prompt radiation.
Nucl. Phys. 60 (1964) p. 378.

11. VAL'SKII G.V. et al.,
Concerning the emission times of γ-quanta as a result of fission.
Sov. At. Energy 18 (1965) p. 279.

12. SKARSVÅG K.,
Time distribution of γ-rays from spontaneous fission of ^{252}Cf.
Nucl. Phys. A153 (1970) p. 82.

13. ARMBRUSTER P. et al.,
Mass dependence of anisotropy and yield of prompt γ-rays in ^{235}U thermal fission.
Physics and chemistry of fission.
Proc. of a symp. Vienna, 28 July - 1 August, 1969.
IAEA, Vienna, 1969, p. 545.

14. ALBINSSON H.,
Yield of prompt gamma radiation in slow-neutron induced fission of ^{235}U as a function of the total fragment kinetic energy. 1971.
(AE-417).

15. BLINOV M.V. et al.,
Angular anisotropy of the gamma quanta accompanying U^{235} fission.
Sov. Phys. JETP 16 (1963) p. 1159.

16. GRAFF G., LAJTAI A., and NAGY L.,
The angular distribution of gamma-rays from the fission of U^{235}.
Physics and chemistry of fission.
Proc. of a symp. Salzburg, 22 - 26 March, 1965.
IAEA, Vienna, 1965. Vol. 2, p. 163.

17. VERBINSKI V.V., WEBER H., and SUND R.E.,
Prompt gamma-rays from ^{235}U (n, f), ^{239}Pu (n, f) and ^{252}Cf (spontaneous fission). (Abstract.)
Physics and chemistry of fission.
Proc. of a symp. Vienna, 28 July - 1 August, 1969.
IAEA, Vienna, 1969, p. 929.

18. ALBINSSON H. and LINDOW L.,
Prompt gamma radiation from fragments in the thermal fission of ^{235}U. 1970.
(AE-398).

19. BECKMAN L., HANSÉN J., and JANSSON R.,
A fast time-of-flight spectrometer.
Nucl. Instr. Methods. 52 (1967) p. 157.

20. GERE E.E. and MILLER G.L.,
A high speed analog pulse divider.
IEEE Trans. Nucl. Sci. NS-11 (1964):3 p. 382.

21. MAIENSCHEIN F.C. et al.,
Gamma-rays associated with fission.
U.N. intern. conf. on peaceful uses of atomic energy.
2. Geneva 1958. Proc. Vol. 15, p. 366.
U.N. Geneva, 1958.

21A. PEELLE R. W. and MAIENSCHEIN F. C.,
Spectrum of photons emitted in coincidence with fission of ^{235}U by thermal neutrons.
Phys. Rev. C. 3 (1971) p. 373.

22. ALBINSSON H.,
To be published.

23. TERRELL J.,
Fission neutron spectra and nuclear temperatures.
Phys. Rev. 113 (1959) p. 527.

24. JOHANSSON S. A. E. and KLEINHEINZ P.,
Gamma-radiation from fission. Alpha-, beta- and gamma-ray spectroscopy.
Ed. by K. Siegbahn. North Holland Publ. Co.
Amsterdam 1965, Vol. 1, p. 805.

25. KAPOOR S. S., RAMANNA R., and RAMA RAO P. N.,
Emission of prompt neutrons in the thermal neutron fission of U^{235}.
Phys. Rev. 131 (1963) p. 283.

26. SKARSVÅG K. and BERGHEIM K.,
Energy and angular distributions of prompt neutrons from slow neutron fission of U^{235}.
Nucl. Phys. 45 (1963) p. 72.

27. BLINOV M. V. et al.,
Dependence of the anisotropy of fission neutron emission on the total kinetic energy of the fragments.
Sov. J. Nucl. Phys. 12 (1971) p. 22.

28. MASLIN E. E., RODGERS A. L., and CORE W. G. F.,
Prompt neutron emission from U^{235} fission fragments.
Phys. Rev. 164 (1967) p. 1520.

29. STAVINSKII V. S.,
On the emission mechanism of prompt fission neutrons.
Sov. Phys. JETP 9 (1959) p. 437.

30. FULLER R. W.,
Dependence of neutron production in fission on rate of charge of nuclear potential.
Phys. Rev. 126 (1962) p. 684.

31. VANDENBOSCH R.,
Dependence of fission fragment kinetic energies and neutron yields on nuclear structure.
Nucl. Phys. 46 (1963) p. 129.

32. TERRELL J.,
Prompt neutrons from fission.
Physics and chemistry of fission.
Proc. of a symp. Salzburg, 22 - 26 March, 1965.
IAEA, Vienna, 1965, Vol. 2, p. 3.

33. ARMBRUSTER P., LABUS H., and REICHELT K.,
Investigation on the primary spins of the ^{235}U fission fragments.
To be published in Z. Naturforschung, March 1971.

34. MAIER-LEIBNITZ H., SCHMITT H. W., and ARMBRUSTER P.,
Average number and energy of gamma-rays emitted as a function of fragment mass in U^{235} thermal-neutron-induced fission.
Physics and chemistry of fission.
Proc. of a symp. Salzburg, 22 - 26 March 1965.
IAEA, Vienna, 1965. Vol. 2, p. 143.

35. MAIER-LEIBNITZ H., ARMBRUSTER P., and SPECHT H. J.,
Prompt and delayed gamma-rays from fission.
Physics and chemistry of fission.
Proc. of a symp. Salzburg, 22 - 26 March 1965.
IAEA, Vienna, 1965, Vol. 2, p. 113.

36. JOHANSSON S. A. E.,
Nuclear octupole deformation and the mechanism of fission.
Nucl. Phys. 22 (1961) p. 529.

37. DONNER W. and GREINER W.,
Octupole vibrations of deformed nuclei.
Z. Physik 197 (1966) p. 440.

38. KRAPPE H. J. and WILLE U.,
Collective model for pear-shaped nuclear.
Nucl. Phys. A124 (1969) p. 641.

39. NEERGÅRD K. and VOGEL P.,
Low-lying octupole states of the doubly even deformed nuclei with $152 \leqq A \leqq 190$.
Nucl. Phys. A145 (1970) p. 33.

FIGURE CAPTIONS

Fig. 1 Block schematic of the electronic equipment.

Fig. 2 The energy spectrum of the uncollimated gamma-rays emitted within 5×10^{-9} s after the fission event.

Fig. 3 The energy spectrum of the gamma radiation from all fragments associated with half-lives of 50 ps and more.

Fig. 4 The low energy part of the spectrum of the gamma radiation from all fragments associated with half-lives of 50 ps and more.

Fig. 5 Gamma-ray energy spectra of the same radiation as in fig. 3 for a number of different masses.

Fig. 6 The relative gamma-ray yield of the energy portion 100 - 230 keV as a function of fragment mass associated with the half-lives of 50 ps and more.

Fig. 7 The relative gamma-ray yield of the energy portion 0.4 - 0.8 MeV as a function of fragment mass associated with half-lives of 50 ps and more.

Fig. 8 The relative gamma-ray yield of the energy portion 1.0 - 1.4 MeV as a function of fragment mass associated with half-lives of 50 ps and more.

Fig. 9 The relative gamma-ray yield of the energy portion 50 - 400 keV as a function of fragment mass associated with half-lives of 50 ps and more.

Fig. 10 Gamma-ray energy spectra of the radiation with a half-life of about 20 ps for a number of different masses.

Fig. 11 Relative gamma-ray yields as function of fragment mass from the radiation shown in fig. 10 and for different energy portions: (a) 0.2 - 2.0 MeV, (b) 0.2 - 0.6 MeV, (c) 0.2 - 0.4 MeV, (d) 0.4 - 0.6 MeV, (e) 0.6 - 0.8 MeV, (f) 0.8 - 1.0 MeV.

Fig. 12 The energy spectrum of the gamma radiation from all fragments associated with half-lives shorther than 10 ps.

Fig. 13 Gamma-ray energy spectra of the radiation with half-lives shorter than 10 ps for some different masses.

Fig. 14 The relative gamma-ray yield of the energy range 0.2 - 2.0 MeV as a function of fragment mass associated with half-lives shorter than 10 ps.

Fig. 15 A portion of the gamma-ray energy spectrum of the uncollimated radiation from the fragment mass regions 104+132.

Fig. 16 The average quantum energy as a function of fragment mass for the energy distribution from 100 - 400 keV associated with half-lives of 50 ps and more.

Fig. 17 The average quantum energy as a function of fragment mass associated with half-lives shorter than 10 ps.

Fig. 18 The average quantum energy as a function of fragment mass associated with half-life of about 20 ps.

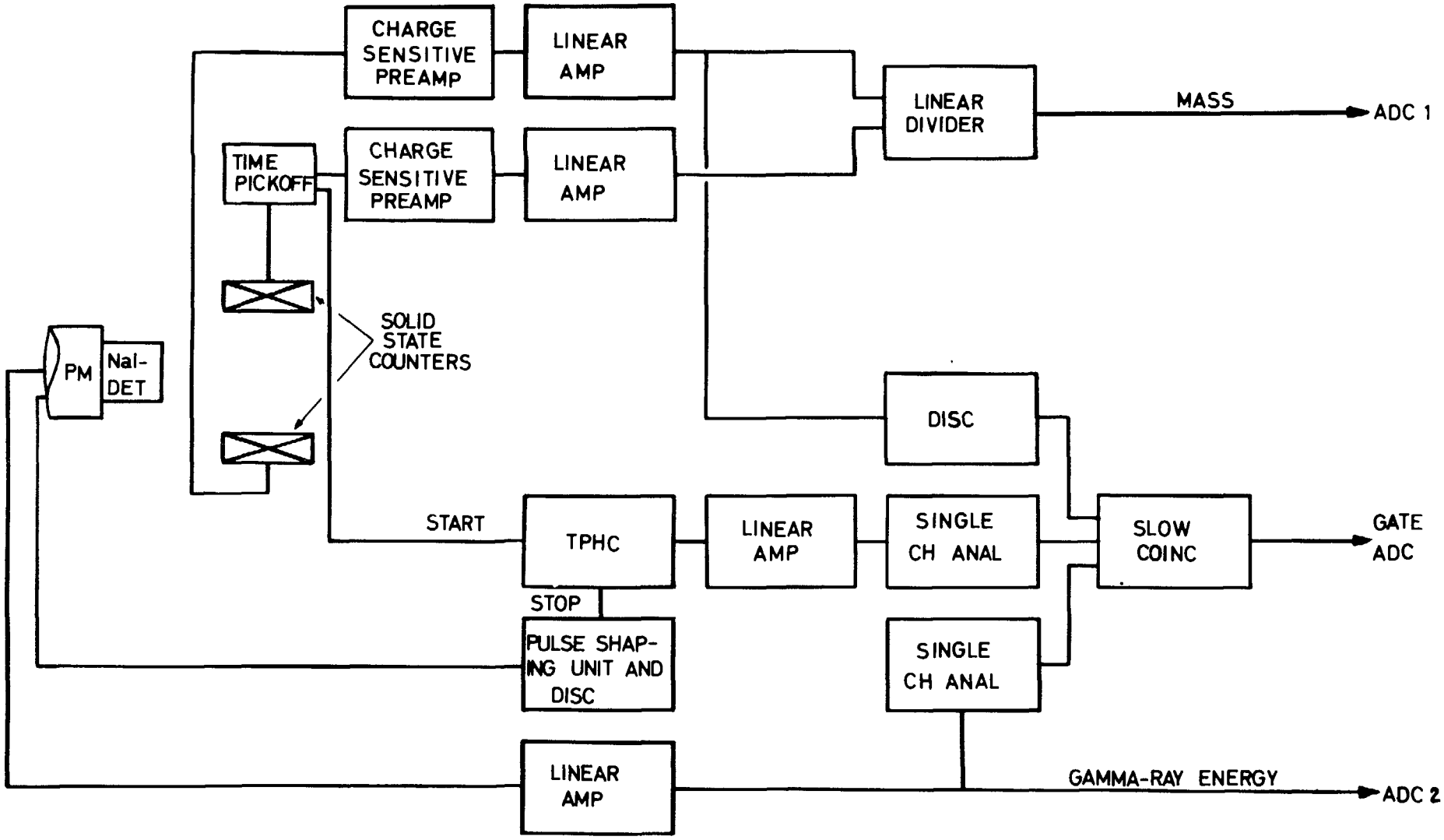
CHARGE SENSITIVE PREAMP
LINEAR AMP
LINEAR DIVIDER
MASS
ADC 1
TIME PICKOFF
CHARGE SENSITIVE PREAMP
LINEAR AMP
SOLID STATE COUNTERS
PM
NaI-DET
DISC
START
TPHC
LINEAR AMP
SINGLE CH ANAL
SLOW COINC
GATE ADC
STOP
PULSE SHAP-ING UNIT AND DISC
SINGLE CH ANAL
LINEAR AMP
GAMMA-RAY ENERGY
ADC 2

Fig 1

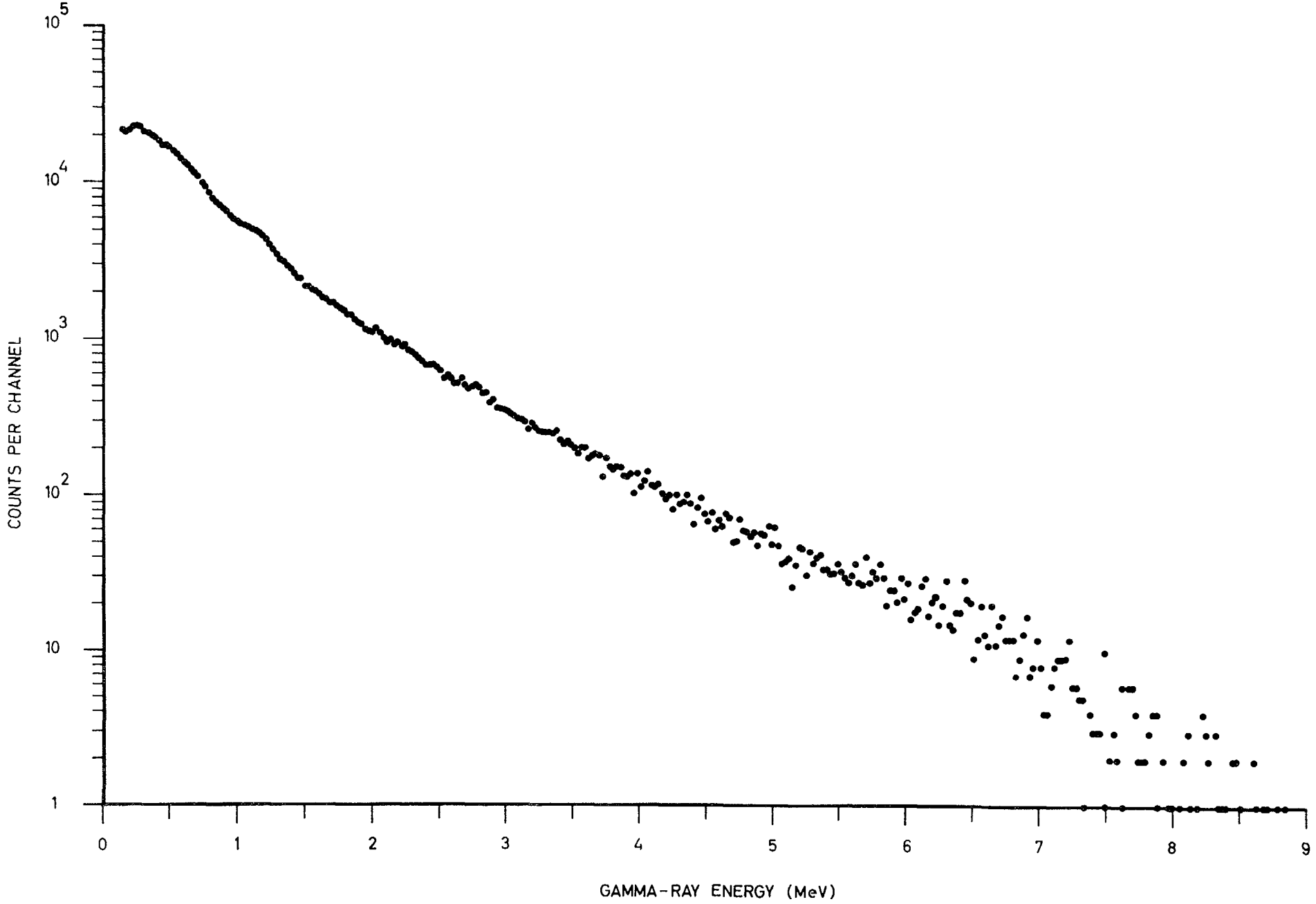
10^5
10^4
10^3
10^2
10
1
COUNTS PER CHANNEL
0
1
2
3
4
5
6
7
8
9
GAMMA-RAY ENERGY (MeV)

Fig 2

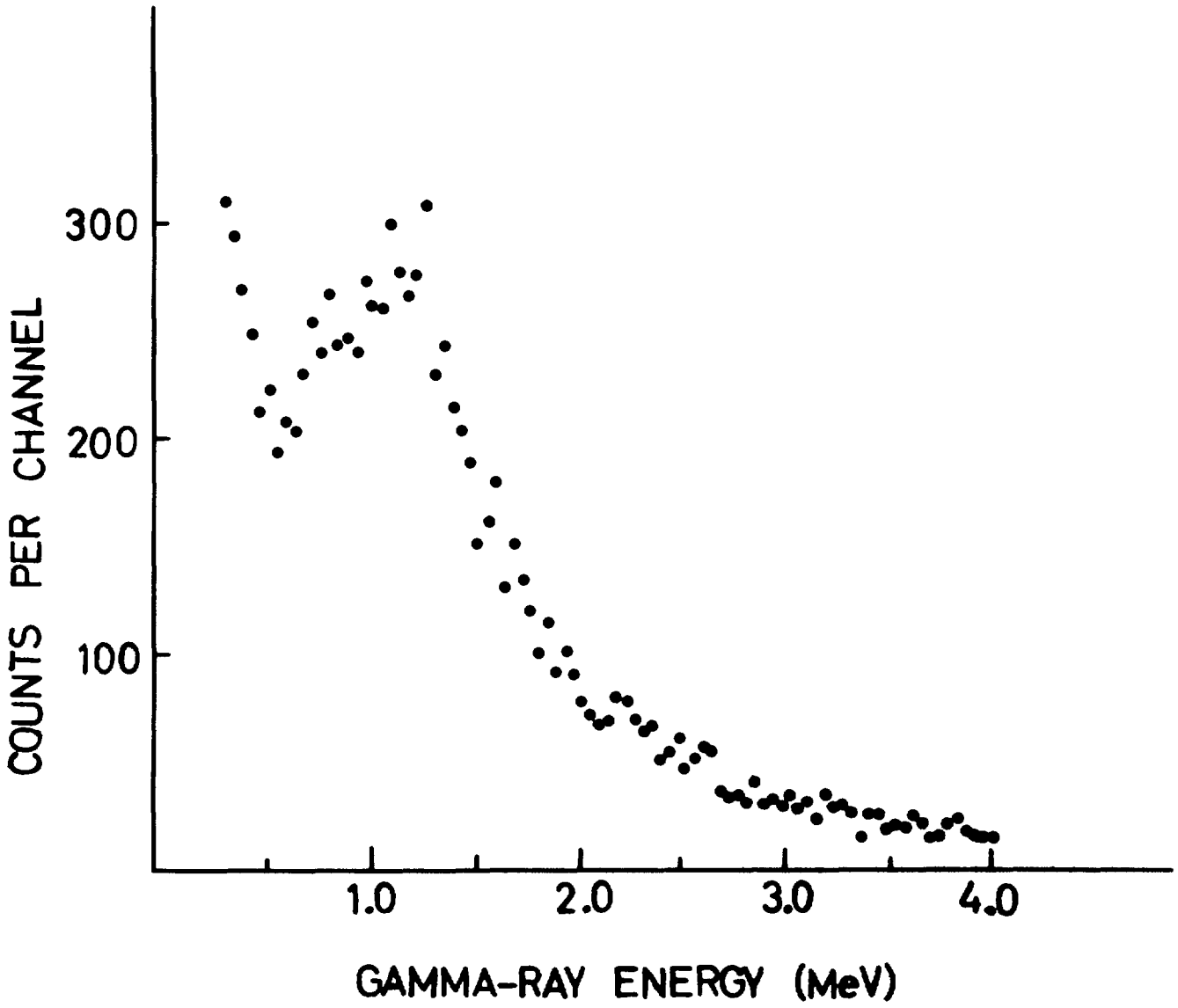
300
200
100
COUNTS PER CHANNEL
1.0
2.0
3.0
4.0
GAMMA-RAY ENERGY (MeV)

Fig 3

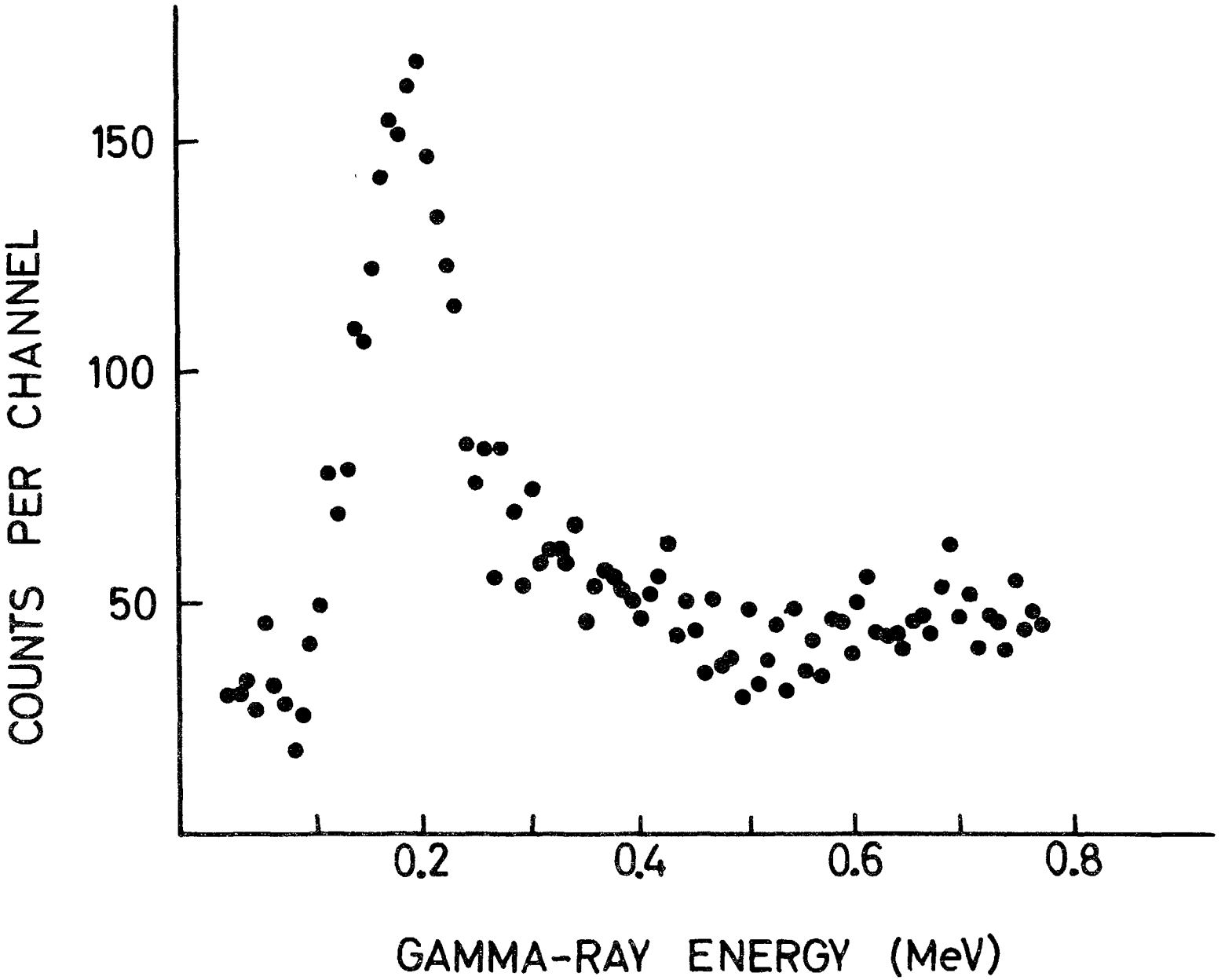

Fig 4

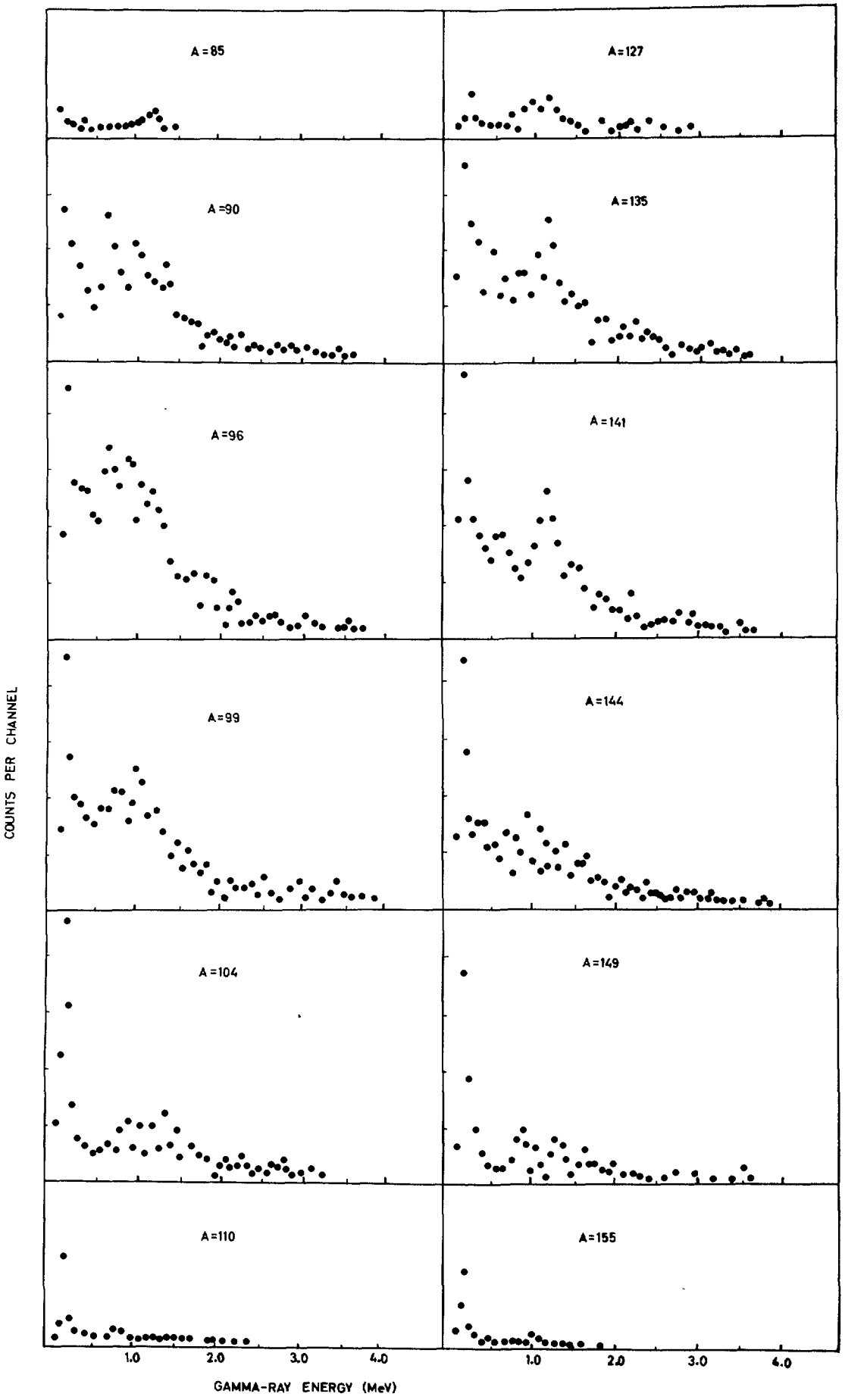
A=85
A=127
A=90
A=135
A=96
A=141
A=99
A=144
A=104
A=149
A=110
A=155
COUNTS PER CHANNEL
1.0
2.0
3.0
4.0
GAMMA-RAY ENERGY (MeV)

Fig 5

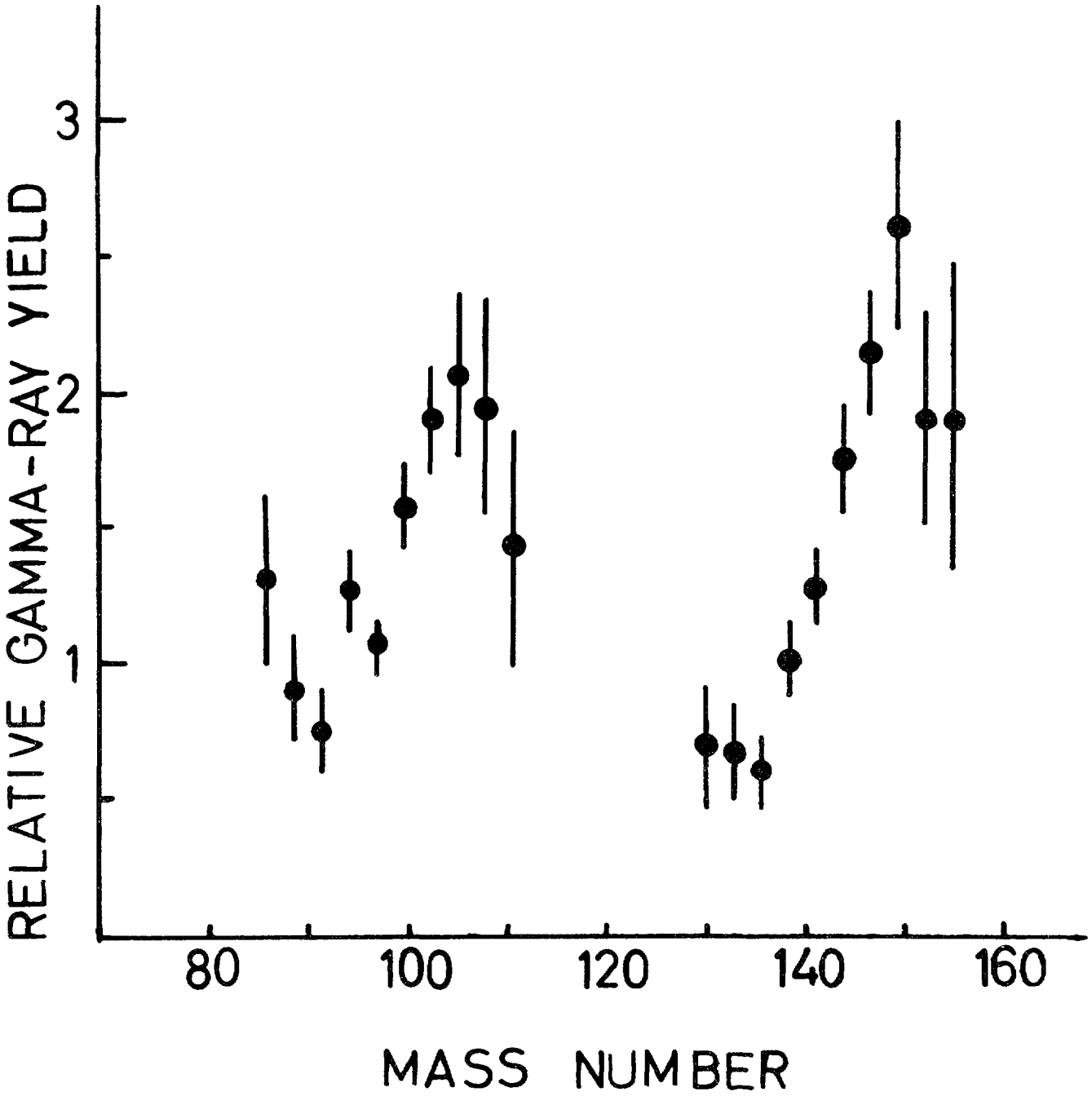

Fig 6

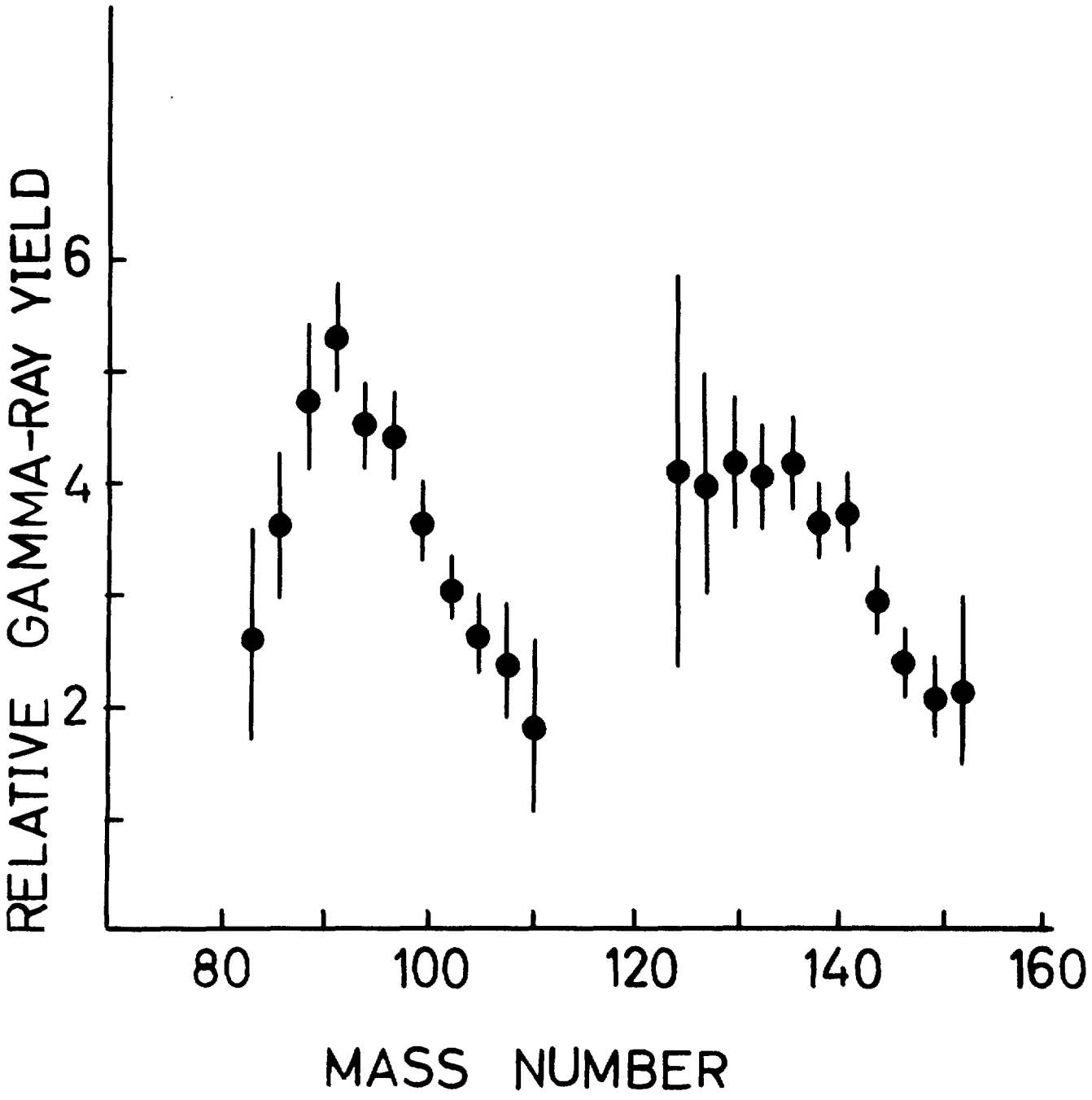

Fig 7

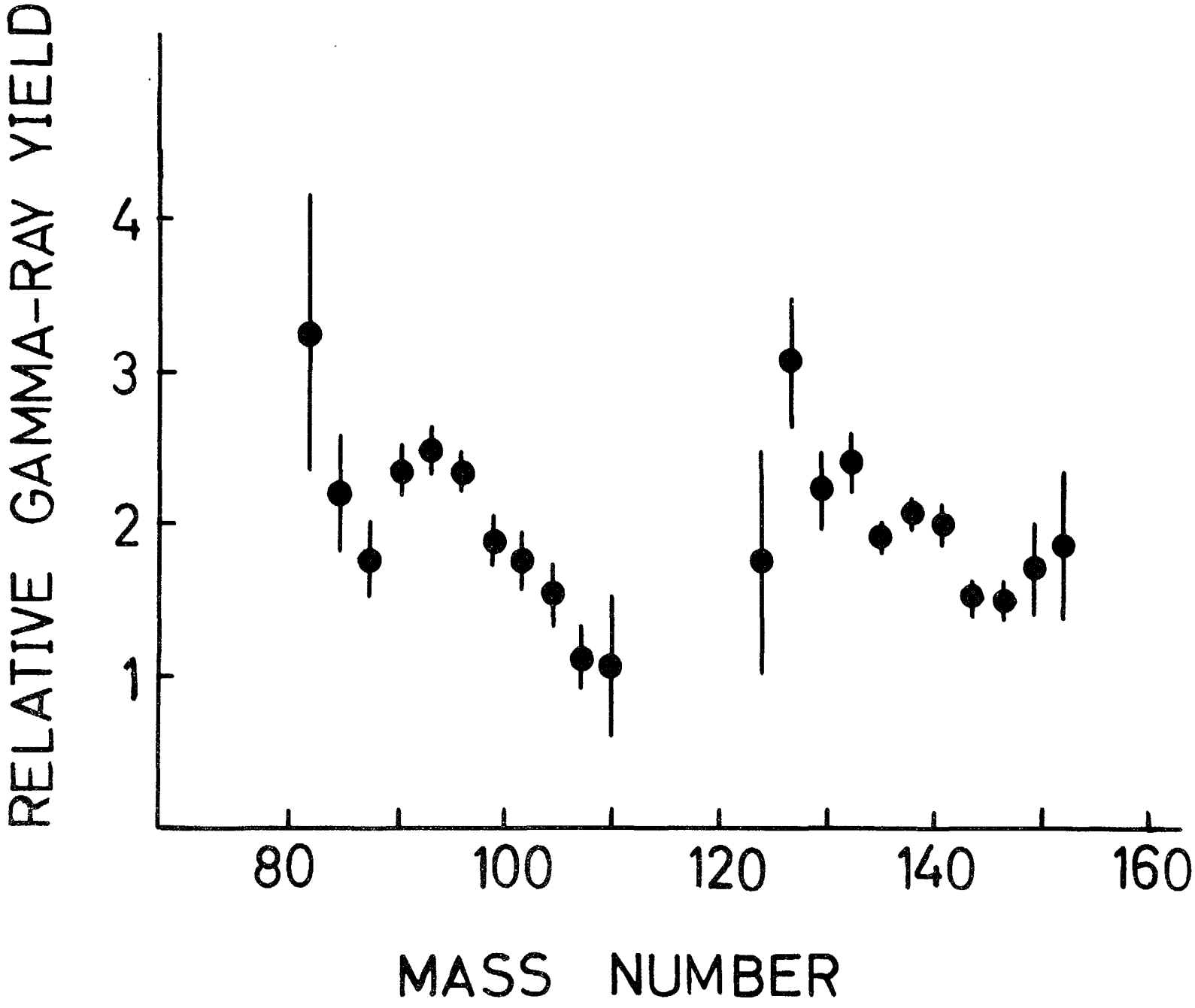

Fig 8

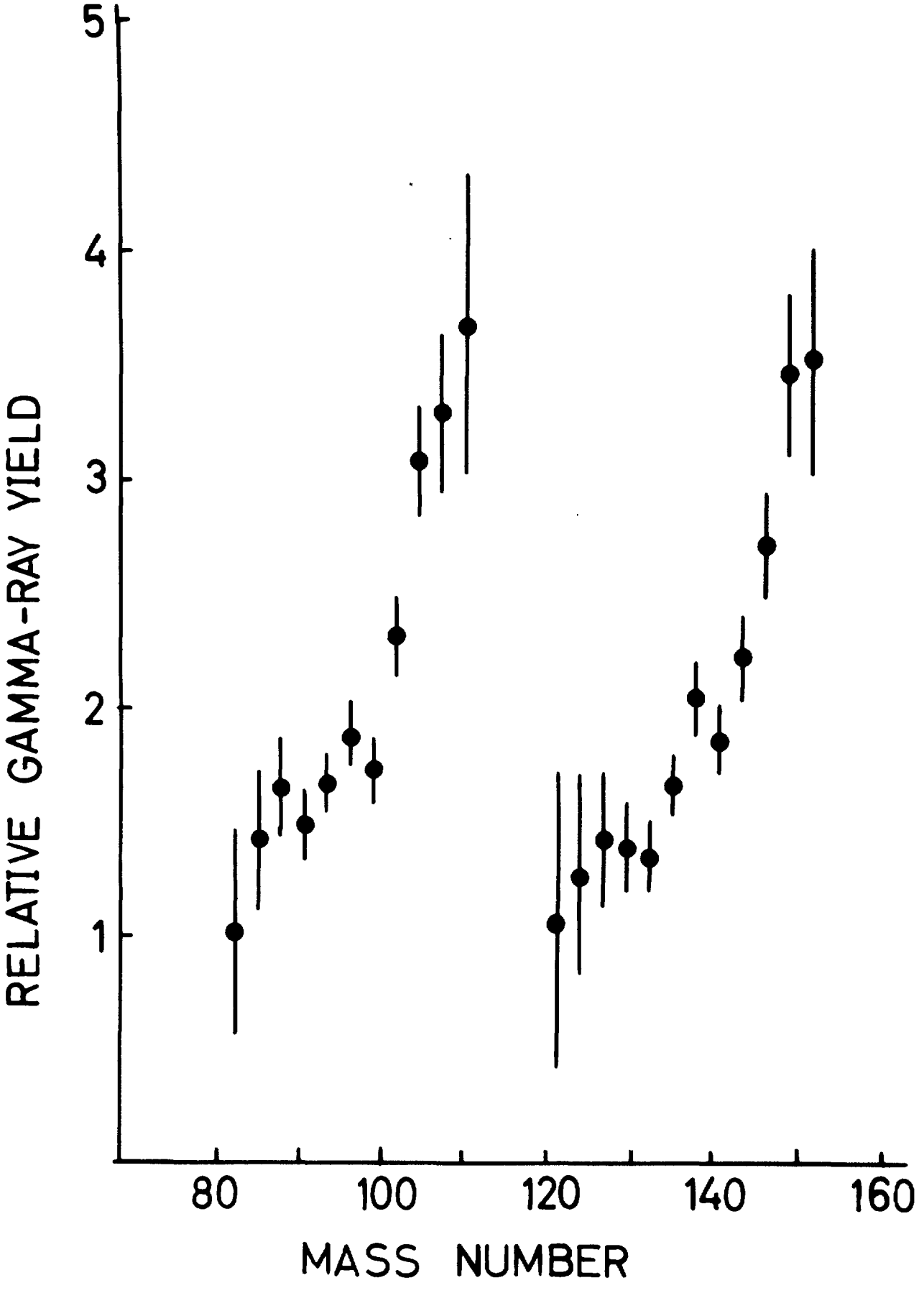
RELATIVE GAMMA-RAY YIELD
5
4
3
2
1
80
100
120
140
160
MASS NUMBER

Fig 9

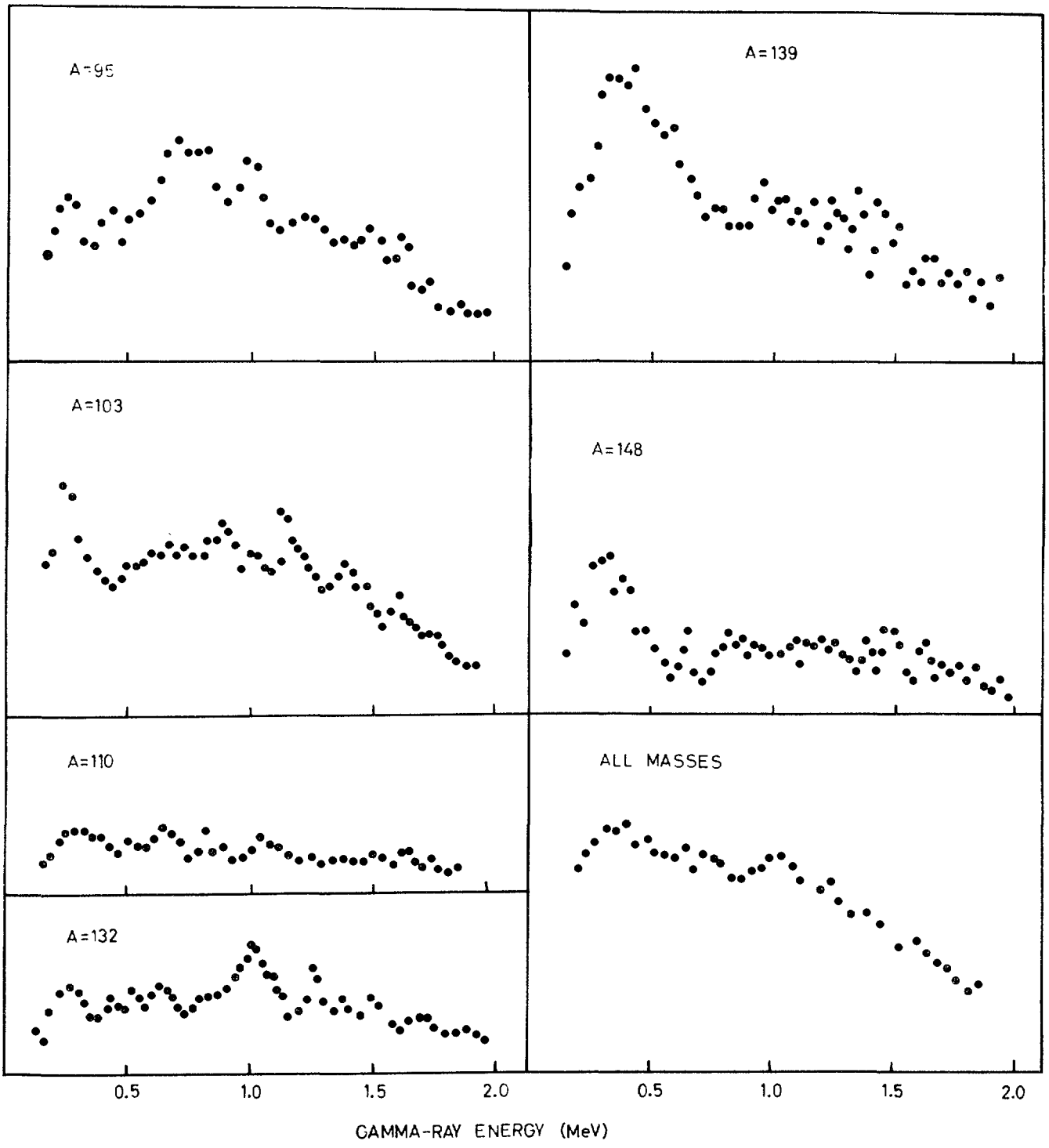
A=95
A=139
A=103
A=148
A=110
ALL MASSES
A=132
0.5
1.0
1.5
2.0
0.5
1.0
1.5
2.0
GAMMA-RAY ENERGY (MeV)

Fig 10

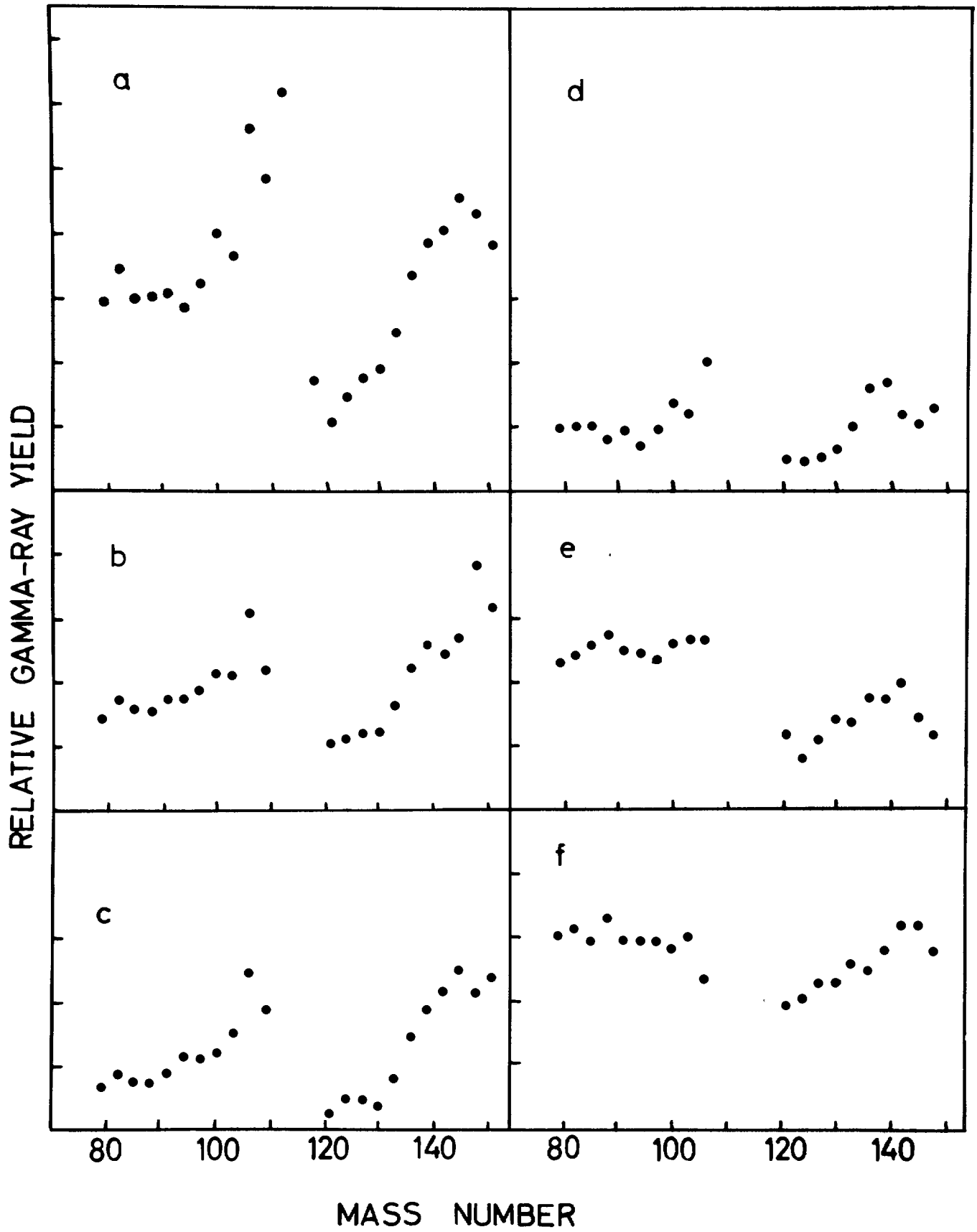
a
b
c
d
e
f
RELATIVE GAMMA-RAY YIELD
80
100
120
140
80
100
120
140
MASS NUMBER

Fig 11

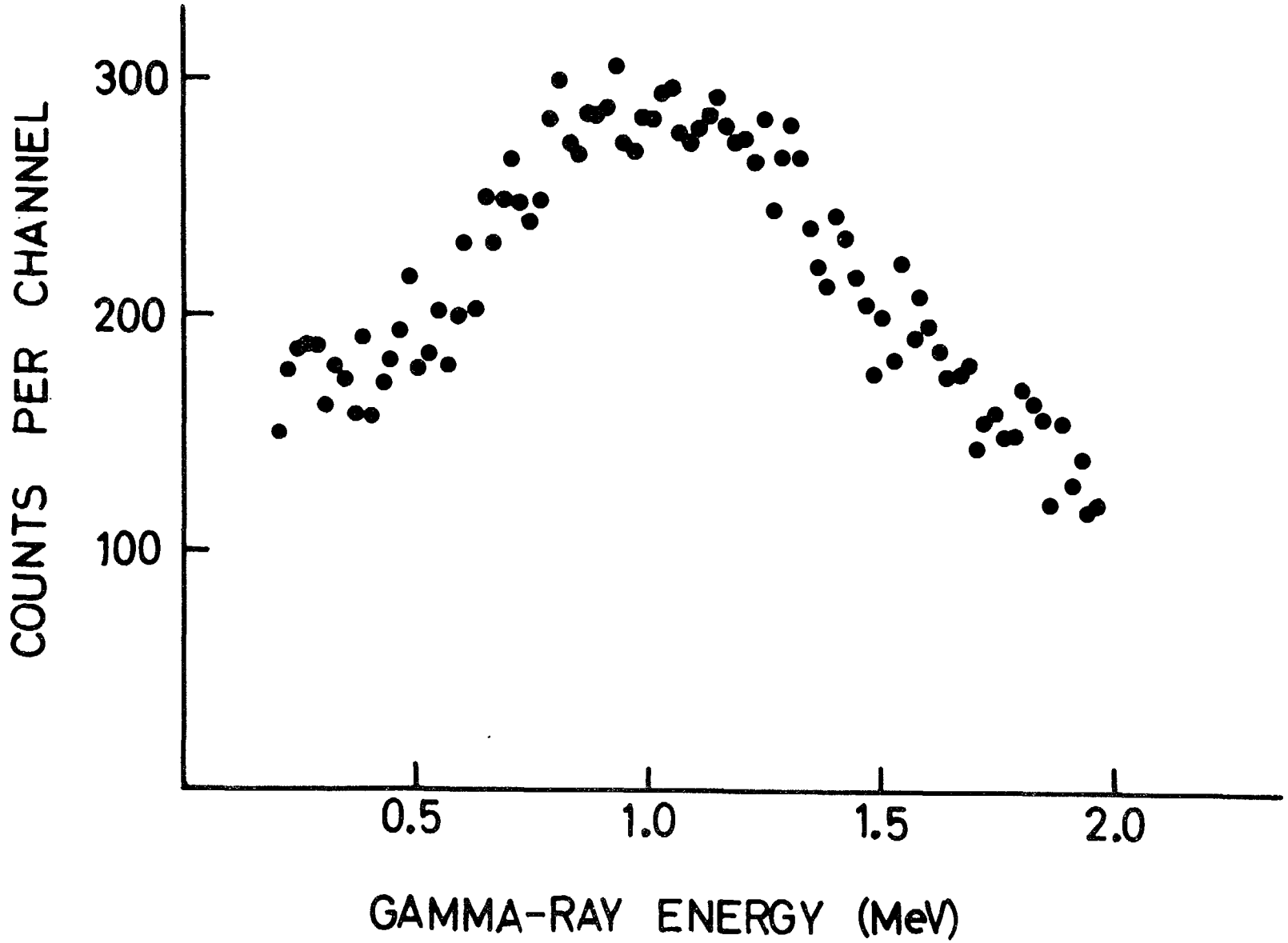
COUNTS PER CHANNEL
300
200
100
0.5
1.0
1.5
2.0
GAMMA-RAY ENERGY (MeV)

Fig 12

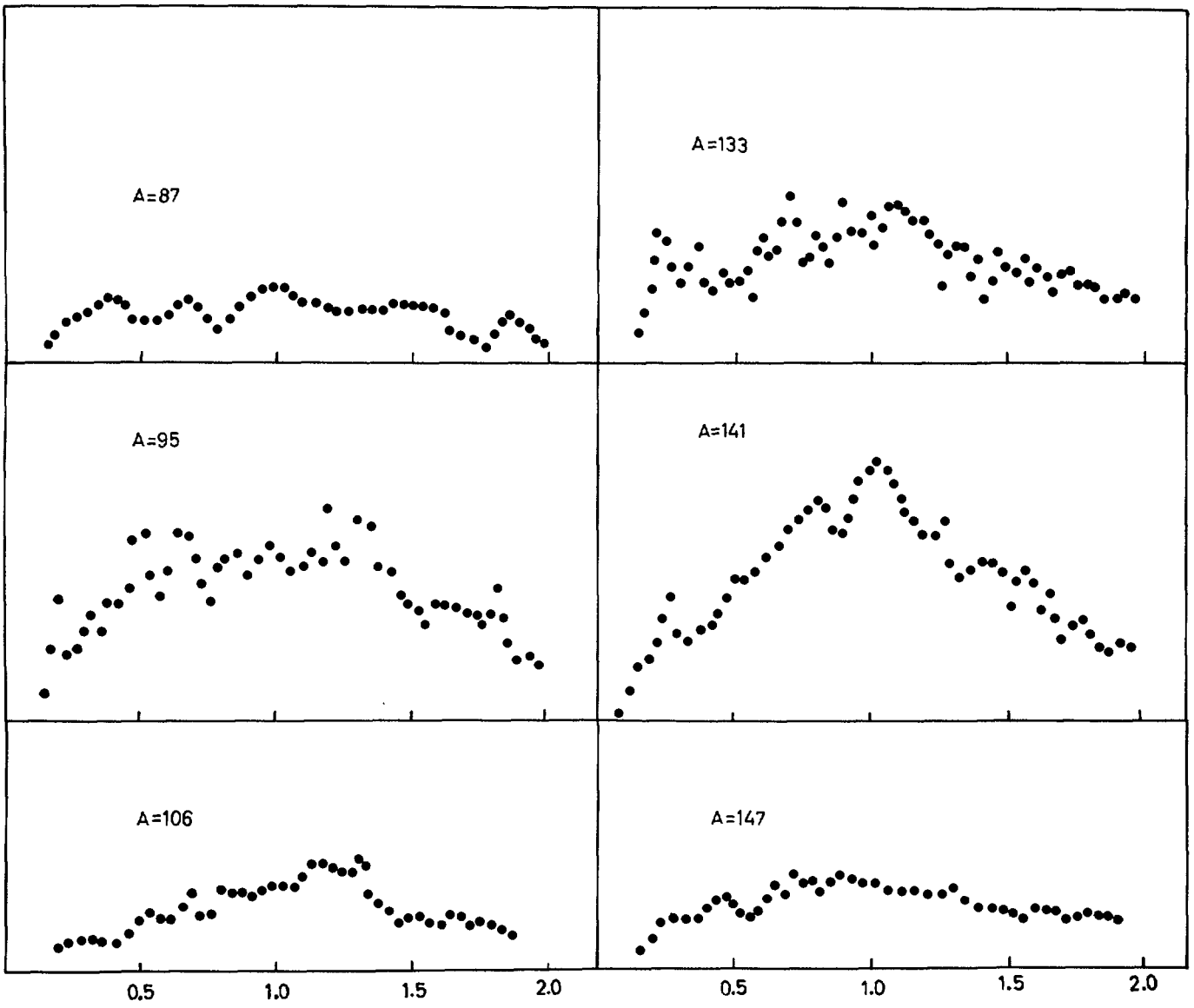
A=87
A=133
A=95
A=141
A=106
A=147
0.5
1.0
1.5
2.0
0.5
1.0
1.5
2.0
GAMMA-RAY ENERGY (MeV)

Fig 13

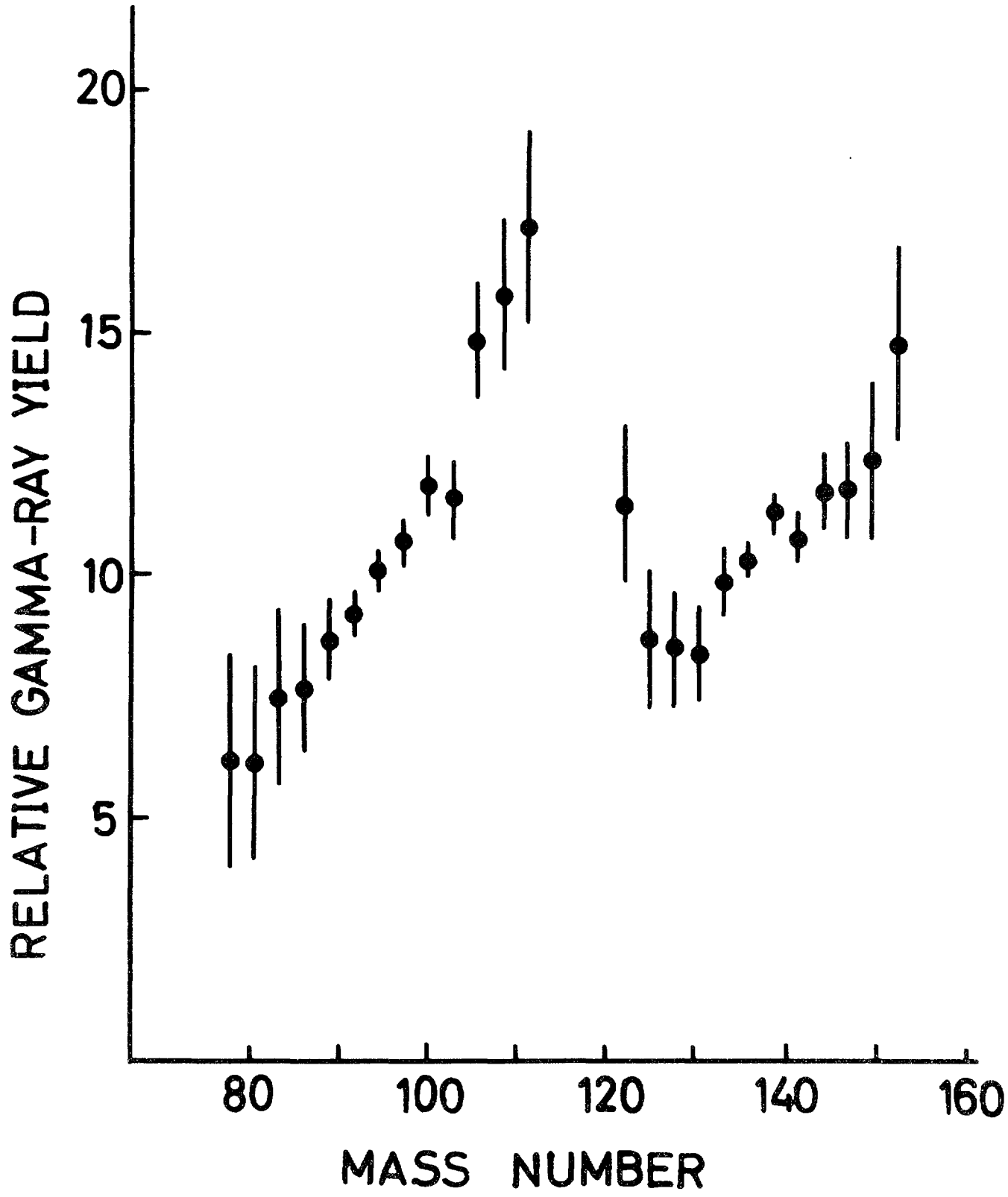
RELATIVE GAMMA-RAY YIELD
20
15
10
5
80
100
120
140
160
MASS NUMBER

Fig 14

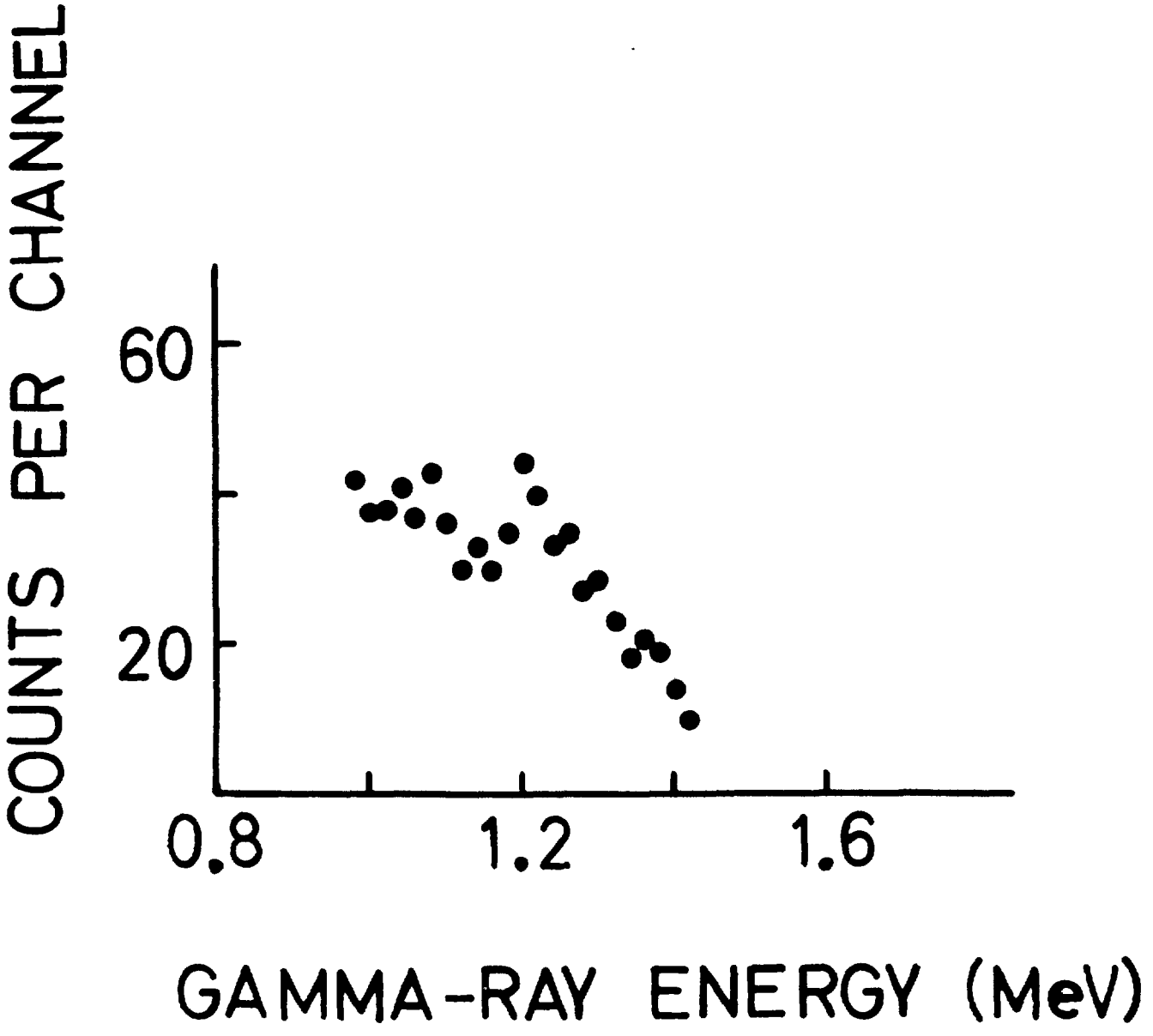

Fig 15

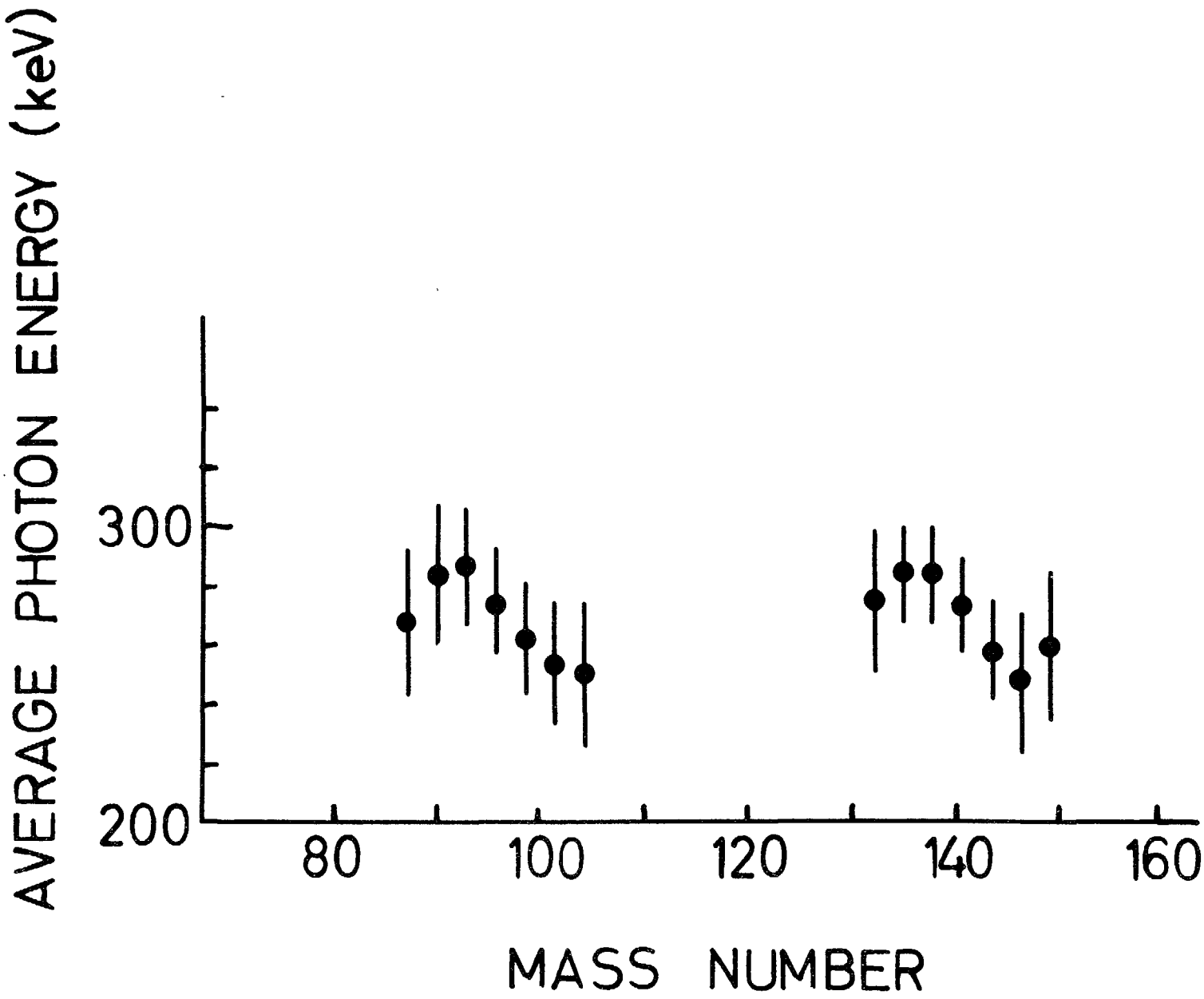
AVERAGE PHOTON ENERGY (keV)
300
200
80
100
120
140
160
MASS NUMBER

Fig 16

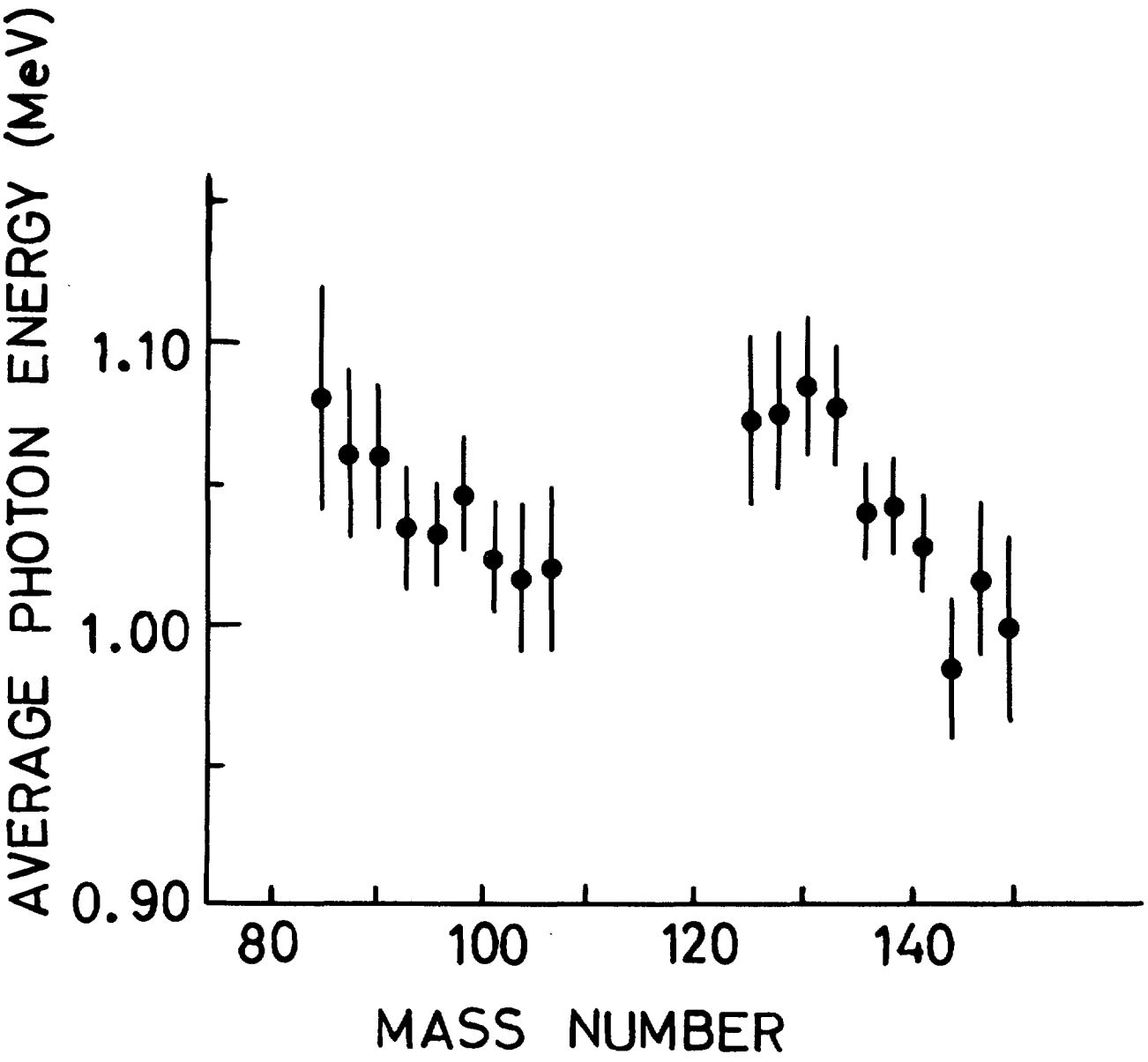
AVERAGE PHOTON ENERGY (MeV)
1.10
1.00
0.90
80
100
120
140
MASS NUMBER

Fig 17

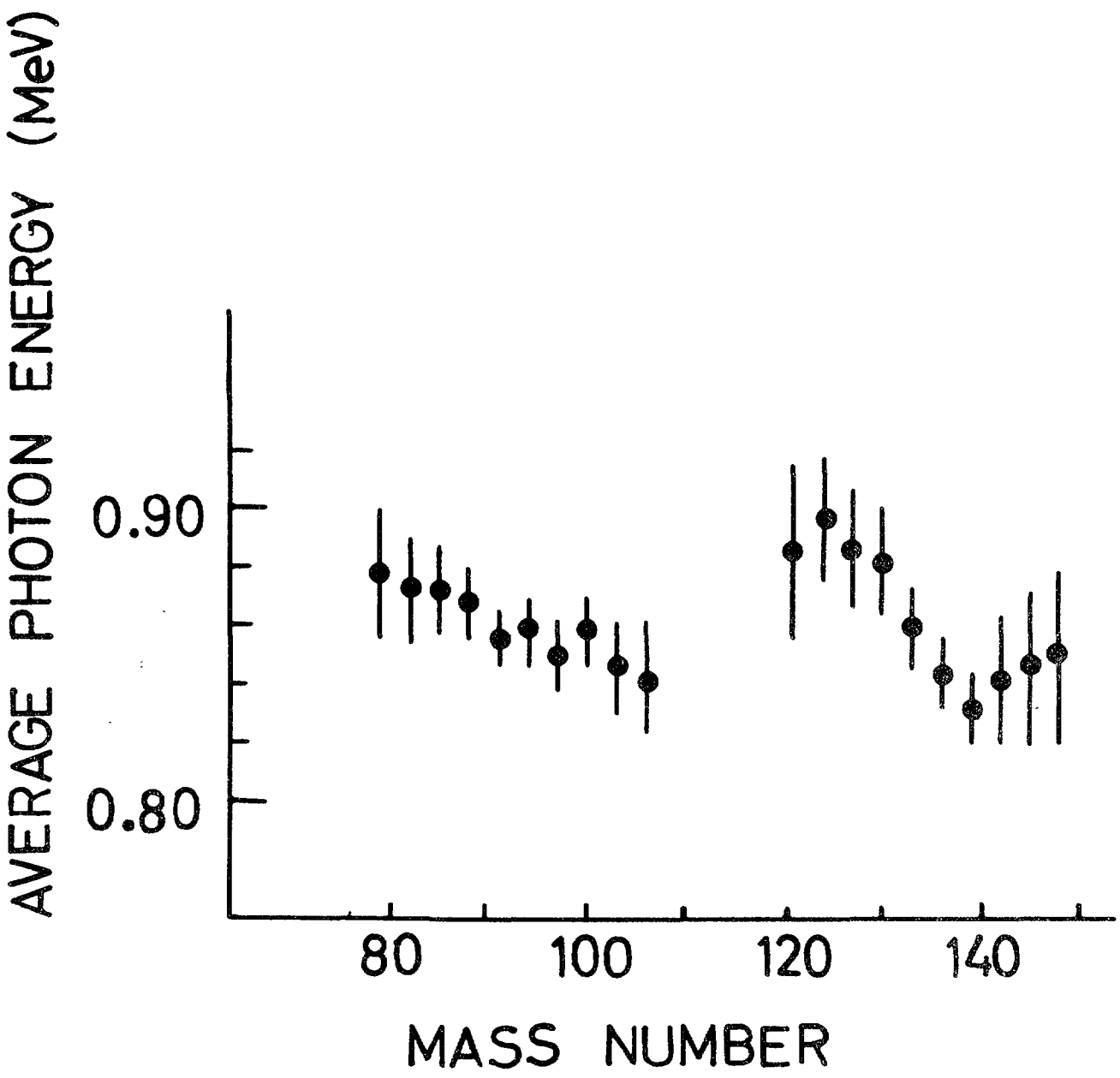

Fig 18

LIST OF PUBLISHED AE-REPORTS

1–350 (See back cover earlier repports.)

351. A determination of the 2 200 m/s absorption cross section and resonance integral of arsenic by pile oscillator technique. By E. K. Sokolowski and R. Bladh. 1969. 14 p. Sw. cr. 10:–.

352. The decay of ^{191}Os. By S. G. Malmskog and A. Bäcklin. 1969. 24 p. Sw. cr. 10:–.

353. Diffusion from a ground level point source experiment with thermoluminescence dosimeters and Kr 85 as tracer substance. By Ch. Gyllander, S. Hollman and U. Widemo. 1969. 23 p. Sw. cr. 10:–.

354. Progress report, FFN, October 1, – September 30, 1968. By T. Wiedling. 1969. 35 p. Sw. cr. 10:–.

355. Thermodynamic analysis of a supercritical mercury power cycle. By A S. Roberts, Jr. 1969. 25 p. Sw. cr. 10:–.

356. On the theory of compensation in lithium drifted semiconductor detectors By A. Lauber. 1969. 45 p. Sw. cr. 10:–.

357. Half-life measurements of levels in ^{75}As. By M. Höjeberg and S. G Malmskog. 1969. 14 p. Sw. cr. 10:–.

358. A non-linear digital computer model requiring short computation time for studies concerning the hydrodynamics of the BWR. By F. Reisch and G. Vayssier. 1969. 38 p. Sw. cr. 10:–.

359. Vanadium beta emission detectors for reactor in-core neutron monitoring. By I. Ö. Andersson and B. Söderlund. 1969. 26 p Sw. cr. 10:–

360. Progress report 1968. Nuclear chemistry. 1969. 38 p. Sw. cr. 10:–.

361. A half-life measurement of the 343.4 keV level in ^{175}Lu. By M. Höjeberg and S. G. Malmskog. 1969. 10 p. Sw. cr. 10:–.

362. The application of thermoluminescence dosimeters to studies of released activity distributions. By B-I. Rudén. 1969. 36 p. Sw. cr. 10:–.

363 Transition rates in ^{161}Dy. By V. Berg and S. G. Malmskog. 1969 32 p Sw. cr. 10:–.

364 Control rod reactivity measurements in the Ägesta reactor with the pulsed neutron method. By K. Björeus. 1969. 44 p. Sw. cr. 10:–.

365. On phonons in simple metals II. Calculated dispersion curves in aluminium. By R. Johnson and A. Westin. 1969. 124 p. Sw. cr. 10:–.

366. Neutron elastic scattering cross sections. Experimental data and optical model cross section calculations. A compilation of neutron data from the Studsvik neutron physics laboratory. By B. Holmqvist and T. Wiedling. 1969. 212 p. Sw. cr. 10:–.

367. Gamma radiation from fission fragments. Experimental apparatus – mass spectrum resolution. By J. Higbie. 1969. 50 p. Sw. cr. 10:–.

368. Scandinavian radiation chemistry meeting, Studsvik and Stockholm, September 17–19, 1969. By H. Christensen. 1969. 34.p. Sw. cr. 10:–.

369. Report on the personnel dosimetry at AB Atomenergi during 1968. By J. Carlsson and T. Wahlberg. 1969 10 p. Sw. cr. 10:–.

370. Absolute transition rates in ^{188}Ir. By S. G. Malmskog and V. Berg. 1969. 16 p. Sw. cr. 10:–.

371. Transition probabilities in the 1/2+(631) Band in ^{235}U. By M. Höjeberg and S. G. Malmskog. 1969. 18 p. Sw. cr. 10:–.

372. E2 and M1 transition probabilities in odd mass Hg nuclei. By V. Berg, A Bäcklin, B Fogelberg and S. G. Malmskog. 1969. 19 p. Sw. cr. 10:–.

373. An experimental study of the accuracy of compensation in lithium drifted germanium detectors. By A. Lauber and B. Malmsten. 1969. 25 p. Sw cr. 10:–.

374. Gamma radiation from fission fragments. By J. Higbie. 1969. 22 p. Sw. cr. 10:–.

375. Fast neutron elastic and inelastic scattering of vanadium. By B. Holmqvist, S. G. Johansson, G. Lodin and T. Wiedling. 1969. 48 p. Sw. cr. 10:–.

376. Experimental and theoretical dynamic study of the Ägesta nucler power station. By P. A. Bliselius, H. Vollmer and F. Åkerhielm. 1969. 39 p Sw. cr. 10:–.

377. Studies of Redox equilibria at elevated temperatures 1. The estimation of equilibrium constants and standard potentials for aqueous systems up to 374°C. By D. Lewis. 1969. 47 p. Sw. cr. 10:–.

378. The whole body monitor HUGO II at Studsvik. Design and operation By L Devell, I. Nilsson and L. Venner. 1970. 26 p. Sw. cr. 10:–.

279. ATOMSPHERIC DIFFUSION. Investigations at Studsvik and Ägesta 1960–1963. By L-E. Hæggblom, Ch. Gyllander and U. Widemo. 1969. 91 p. Sw cr. 10:–.

380. An expansion method to unfold proton recoil spectra. By J. Kockum. 1970. 20 p. Sw. cr. 10:–.

381. The 93.54 keV lever ^{91}Sr, and evidence for 3-neutron states above N=50. By S. G. Malmskog and J. McDonald 1970. 24 p. Sw. cr. 10:–.

382. The low energy level structure of ^{191}Ir. By S. G. Malmskog, V. Berg, A. Bäcklin and G Hedin. 1970. 24 p Sw cr. 10:–.

383. The drinking rate of fish in the Skagerack and the Baltic. By J. E. Larsson. 1970. 16 p. Sw. cr. 10:–.

384. Lattice dynamics of Nacl, KCl, RbCl and RbF. By G. Raunio and S. Rolandson. 1970. 26 p. Sw. cr. 10:–.

385. A neutron elastic scattering study of chromium, Iron and nickel in the energy region 1.77 to 2.76 MeV. By B. Holmqvist, S. G. Johansson, G. Lodin, M Salama and T. Wiedling. 1970. 26 p. Sw. cr. 10:–.

386. The decay of bound isobaric analogue states in ^{28}Si and ^{32}Si using (d. nγ) reactions. By L. Nilsson, A Nilsson and I. Bergqvist. 1970. 34 p. Sw. cr. 10–.

387. Transition probabilities in ^{188}Os. By S. G. Malmskog, V. Berg and A. Bäcklin. 1970 40 p. Sw. cr. 10:–.

388. Cross sections for high-energy gamma transition from MeV neutron capture in ^{206}Pb. By I. Bergqvist, B. Lundberg and L. Nilsson. 1970. 16 p. Sw. cr. 10:–.

389. High-speed, automatic radiochemical separations for activation analysis in the biological and medical research laboratory. By K. Samsahl. 1970. 18 p. Sw. cr. 10:–.

390. Use of fission product Ru-106 gamma activity as a method for estimating the relative number of fission events in U-235 and Pu-239 in low-enriched fuel elements. By R. S. Forsyth and W. H. Blackadder. 1970. 26 p. Sw. cr. 10:–.

391. Half-life measurements in ^{134}I. By V. Berg and A. Höglund. 1970. 16 p Sw. cr. 10:–.

392. Measurement of the neutron spectra in FRO cores 5, 9 and PuB-5 using resonance sandwich detectors. By T. L. Andersson and M. N. Qazi. 1970. 30 p. Sw. cr. 10:–.

393. A gamma scanner using a Ge(Li) semi-conductor detector with the possibility of operation in anti-coincidence mode. By R. S. Forsyth and W. H. Blackadder. 1970. 22 p. Sw. cr. 10:–.

394. A study of the 190 keV transition in ^{141}La. By B. Berg, Å. Höglund and B. Fogelberg. 1970 22 p. Sw cr. 10:–.

395 Magnetoacoustic waves and instabilities in a Hall-effect-dominiated plasma. By S. Palmgren 1970. 20 p Sw. cr. 10:–.

396. A new boron analysis method. By J. Weitman, N. Dåverhög and S. Farvolden. 1970 26 p. Sw. cr. 10:–.

397. Progress report 1969. Nuclear chemistry. 1970. 39 p. Sw. cr. 10:–.

398. Prompt gamma radiation from fragments in the thermal fission of ^{235}U. By H. Albinsson and L. Lindow. 1970. 48 p. Sw. cr. 10:–.

399. Analysis of pulsed source experiments performed in copper-reflected fast assemblies. By J. Kockum. 1970. 32 p. Sw. cr. 10:–.

400. Table of half-lives for excited nuclear levels. By S. G. Malmskog. 1970. 33 p. Sw. cr. 10:–.

401. Needle type solid state detectors for in vivo measurement of tracer activity. By A. Lauber, M. Wolgast. 1970. 43 p. Sw. cr. 10:–.

402. Application of pseudo-random signals to the Ägesta nuclear power station By P-Å. Bliselius. 1970. 30 p. Sw. cr. 10:–.

403 Studies of redox equilibria at elevated temperatures 2. An automatic divided-function autoclave and cell with flowing liquid junction for electrochemical measurements on aqueous systems. By. K. Johnsson, D. Lewis and M. de Pourbaix. 1970. 38 p. Sw. cr. 10:–.

404. Reduction of noise in closed loop servo systems. By K. Nygaard. 1970. 23 p Sw. cr. 10:–

405. Spectral parameters in water-moderated lattices. A survey of experimental data with the aid of two-group formulae. By E. K. Sokolowski. 1970. 22 p. Sw. cr. 10:–.

406. The decay of optically thick helium plasmas, taking into account ionizing collisions between metastable atoms or molecules. By J. Stevefelt. 1970. 18 p. Sw. cr. 10:–.

407. Zooplankton from Lake Magelungen, Central Sweden 1960-63. By E. Almquist. 1970. 62 p. Sw. cr. 10:–.

408. A method for calculating the washout of elemental iodine by water sprays. By E. Bachofner and R. Hesböl. 1970. 24 p. Sw. cr. 10:–.

409. X-ray powder diffraction with Guinier–Hägg focusing cameras. By A. Brown. 1970. 102 p. Sw. cr. 10:–.

410. General physic section Progress report. Fiscal year 1969/70. By J. Braun. 1970. 92 p. Sw. cr. 10:–.

411. In-pile determination of the thermal conductivity of UO_2 in the range 500–2 500 degrees centigrade. By J-Å Gyllander. 1971. 70 p. Sw. cr. 10:–.

412. A study of the ring test for determination of transverse ductility of fuel element canning. By G. Anevi and G. Östberg. 1971. 17 p. Sw. cr. 15:–.

413. Pulse radiolysis of Aqueous Solutions of aniline and substituted anilines. By H. C. Christensen. 1971. 40 p. Sw. cr. 15:–.

414. Radiolysis of aqueous toluene solutions. By H. C. Christensen and R. Gustafson. 1971. 20 p. Sw. cr. 15:–.

415. The influence of powder characteristics on process and product parameters in UO_2 pelletization. By U. Runfors. 1971. 32 p. Sw. cr. 15:–.

416. Quantitative assay of Pu239 and Pu240 by neutron transmission measurements. By E. Johansson. 1971. 26 p. Sw. cr 15:–.

417. Yield of prompt gamma radiation in slow-neutron induced fission of ^{235}U as a function of the total fragment kinetic energy. By H. Albinsson. 1971. 38 p. Sw. cr. 15:–.

418. Measurements of the spectral light emission from decaying high pressure helium plasmas. By J. Stevefelt and J. Johansson. 1971. 48 p. Sw. cr. 15:–.

419. Progress report 1970. Nuclear chemistry. 1971. 32 p. Sw. cr. 15:–.

420. Energies and yields of prompt gamma rays from fragments in slow-neutron induced fission of ^{235}U. By H. Albinsson. 1971. 56 p. Sw. cr. 15:–.

List of published AES-reports (In Swedish)

1. Analysis by means of gamma spectrometry. By D. Brune. 1961. 10 p. Sw. cr. 6:–.
2. Irradiation changes and neutron atmosphere in reactor pressure vessels-some points of view. By M. Grounes 1962. 33 p. Sw. cr. 6:–.
3. Study of the elongation limit in mild steel. By G. Östberg and R. Attermo. 1963. 17 p. Sw cr. 6:–.
4. Technical purchasing in the reactor field. By Erik Jonson. 1963. 64 p. Sw. cr. 8:–.
5 Ägesta nuclear power station. Summary of technical data, descriptions, etc for the reactor. By B. Lilliehöök. 1964. 336 p. Sw. cr. 15:–.
6 Atom Day 1965. Summary of lectures and discussions. By S. Sandström. 1966 321 p. Sw cr. 15:–.
7 Building materials containing radium considered from the radiation protection point of view. By Stig O. W. Bergström and Tor Wahlberg. 1967. 26 p. Sw. cr. 10:–

Additional copies available from the Library of AB Atomenergi, Fack, S-611 01 Nyköping 1, Sweden.

EOS-tryckerierna, Stockholm 1971